

Title	Towards Unquenched Holographic Magnetic Catalysis
Creators	Filev, Veselin G. and Zoakos, Dimitrios
Date	2011
Citation	Filev, Veselin G. and Zoakos, Dimitrios (2011) Towards Unquenched Holographic Magnetic Catalysis. (Preprint)
URL	https://dair.dias.ie/id/eprint/522/
DOI	DIAS-STP-11-03

Towards Unquenched Holographic Magnetic Catalysis

Veselin Filev *

*Max-Planck-Institut für Physik (Werner-Heisenberg-Institut)
Föhringer Ring 6, 80805 München, Germany*

ℰ

*School of Theoretical Physics
Dublin Institute for Advanced Studies
10 Burlington Road, Dublin 4, Ireland*

Dimitrios Zoakos †

*Centro de Física do Porto ℰ Departamento de Física e Astronomia
Faculdade de Ciências da Universidade do Porto
Rua do Campo Alegre 687, 4169-007 Porto, Portugal*

ABSTRACT: We propose a string dual to the $SU(N_c)$ $\mathcal{N} = 4$ SYM coupled to N_f massless fundamental flavors in an external magnetic field. The flavors are introduced by homogeneously smeared N_f D7-branes and the external magnetic field via a non-trivial Kalb-Ramond B -field. Our solution is perturbative in a parameter that counts the number of internal flavor loops. In the limit of vanishing B -field the background reduces to the supersymmetric one obtained in hep-th/0612118. We introduce an additional probe D7-brane and in the supersymmetric limit of vanishing B -field perform a holographic renormalization of its “on-shell” action. We consider also non-supersymmetric probes with fixed worldvolume gauge field corresponding to a magnetic field coupled only to the fundamental fields of the probe brane. We study the influence of the backreacted flavors on the effect of dynamical mass generation. Qualitatively the physical picture remains unchanged. In the next step we consider the case when the magnetic field couples to both the backreacted and the probe fundamental degrees of freedom. At sufficiently strong magnetic field the meson spectrum signals an instability of the probe D7-brane, which we interpret as reflecting an instability of the supergravity background.

*E-mail address: filev@mppmu.mpg.de

†E-mail address: dimitrios.zoakos@fc.up.pt

Contents

1. Introduction	2
2. Constructing the background	4
2.1 Ansatz	5
2.2 Effective action and the equations of motion	6
2.3 Perturbative solution	8
2.4 Validity of the perturbative solution	10
3. Probing the supersymmetric background	11
3.1 Holographic renormalization	12
3.2 D7-brane probe with fixed $U(1)$ -gauge field.	15
4. Probing the fully backreacted background	17
4.1 Classical embeddings	18
4.2 Meson spectrum	22
4.2.1 Quadratic fluctuations.	22
4.2.2 Fluctuations along χ	24
5. Conclusions	25
6. Acknowledgments	27
A. Equations of motion	28
B. Technical details	29
B.1 Exact On-Shell Action	30
B.2 The Function h	30

1. Introduction

In recent years an exciting area of theoretical physics has been unveiled through the discovery of the AdS/ CFT correspondence and its numerous generalizations, [1]. Holographic techniques have proven a powerful analytic tool in studying the qualitative properties of strongly interacting physical systems with applications ranging from describing the physics of strongly interacting quark gluon plasmas to modeling collective condensed matter phenomena such as superconductivity and superfluidity.

Despite the success of the AdS/CFT correspondence in studying holographic gauge theories, namely field theories with known dual supergravity backgrounds, there are many realistic theories of great phenomenological importance, such as QCD, which do not have an explicit holographic dual. This is the main reason of the limited direct quantitative applications of the correspondence. However, it turns out that under extreme external control parameters, such as: temperature, chemical potential and external electromagnetic fields, different gauge theories exhibit similar properties. Therefore it is natural to apply holographic techniques to study phenomena which are known to be of universal nature.

One such phenomenon is the magnetic catalysis of mass generation. At weak coupling it has been extensively studied using the conventional perturbative field theoretic techniques [2]. A holographic study of this effect has been performed in [3], where the case of flavored $\mathcal{N} = 4$ Yang-Mills theory has been explored. Further holographic studies of this phenomenon have been addressed by numerous authors ¹ (for a comprehensive review of the literature look at ref. [4]). At present all such studies are in the limit of the so called “quenched” approximation when the number of fundamental fields N_f is much smaller than the number of color degrees of freedom N_c . On the gravity side this corresponds to the probe limit for the flavor D7-branes.

In this paper we undertake first steps towards a holographic description of the phenomenon of magnetic catalysis of mass generation beyond the “quenched” approximation. This suggests the construction of a supergravity background with a fully backreacted set of flavor branes coupled to a non-vanishing B -field. This construction amounts to a non-supersymmetric background.

Ideally such a background would correspond to a set of fully localized flavor branes. The gravity dual of a field theory with unquenched flavor is coming through the solution of the equations of motion with brane sources. It is the presence of these sources which typically modify the Bianchi identities and through their contribution to the energy-momentum tensor, the Einstein equations also. If the flavor branes are localized, the sources contain Dirac delta functions and, as a consequence, solving the equations of motion is, in general, a difficult task. In the context of the AdS/CFT correspondence, the search for localized solutions was initiated in [6], where the D3-D7 intersections were discussed, while a lot of progress was reported in subsequent years, (see e.g. [7]).

We could overcome the technical difficulties of localized flavor brane embeddings by considering configurations which are partially smeared ² along appropriately chosen compact directions. Supersymmetric backgrounds corresponding to partially smeared Karch-Katz like embeddings, [9], have been constructed in [10]. In general these backgrounds possess a hollow cavity in the bulk of the

¹For a concise review in the case of holographic duals to the Dp/Dq-brane intersections look at ref. [5].

²For a detailed review on the smearing approach see [8].

geometry where the supergravity solution is sourced solely by the color branes. The radius of this cavity is related to the bare mass of the fundamental flavors [11]. In the limit of vanishing bare mass the cavity shrinks to the radius of the compact part of the geometry and the supergravity background has an essential singularity at the origin of the non-compact part of the geometry. In both cases the dilaton field diverges at large radial distances. This corresponds to the Landau pole that the dual field theory develops in the UV, due to its positive beta function $\beta(\lambda) \propto N_f/N_c$.

One can imagine that a non-supersymmetric background interpolating between the supersymmetric backgrounds corresponding to massless flavors in the UV and massive flavors in IR would describe a dynamical mass generation. The radius of the hollow cavity would correspond to the dynamically generated constituent mass of the fundamental flavors.

A promising framework for the construction of such a geometry has been developed in [12]. In this paper, a ten dimensional black-hole solution dual to the non conformal plasma of $\mathcal{N} = 4$ Yang-Mills coupled to $N_f \gg 1$ massless flavors has been presented³. The D7 flavor branes are smeared homogeneously and extend along the radial direction up to the black hole horizon. The smearing procedure reduces the flavor symmetry group from $U(N_f)$ to $U(1)^{N_f}$ and allows for a simple way to account for the backreaction of the flavor branes. This in turn allows one to explore the “unquenched” regime of the dual field theory. In the zero temperature limit, the resulting backgrounds coincide with those found in [15].⁴ More precisely, the authors of [12] consider the smearing of a general non-supersymmetric “fiducial” embedding of the flavor brane for the purpose of obtaining a perturbative non-extremal black hole solution. However it turns out that obtaining even a perturbative solution in the general case is technically too difficult and the authors obtain a perturbative finite temperature solution for the particular case of massless flavors (when the “fiducial” embedding is trivial).

In this paper we will construct a perturbative non-supersymmetric background with a non-vanishing B -field, which corresponds to an external magnetic field coupled to the fundamental degrees of freedom of the dual gauge theory. Following the approach of [12] we will consider the case when the “fiducial” embedding is trivial. Note that the results of the probe limit case considered in [3], show that this embedding is unstable since it corresponds to vanishing constituent mass of the fundamental flavors. In the probe limit this instability is present for any non-vanishing value of the external magnetic field. Therefore one may expect that the background obtained by smearing such unstable embeddings would also be unstable. However the effect of backreaction is that the theory develops a Landau pole. This suggests the existence of an extra energy scale in addition to the energy scale associated to the external magnetic field. Therefore we may expect that the supergravity background would be characterized by a non-zero critical value of the B -field (H_{cr}) below which the background is stable. Our studies on the stability of the background using a probe D7-brane confirm this expectation.

Let us summarize the content of our work:

In Section 2 we introduce useful notation and the supergravity ansatz that is appropriate for the description of the backreacted supergravity background discussed above. We proceed by construct-

³All the hydrodynamic transport coefficients of the model were analyzed in [13], while the addition of a finite baryon density was presented in [14]

⁴Other solutions employing the smearing technique appear in [16].

ing an effective one dimensional action and obtaining the supergravity equations of motion. After that we solve those equations perturbatively to first order an appropriate small parameter, namely $\epsilon_* \propto \lambda_* \frac{N_f}{N_c}$. We are able to present our solution in a closed form. In the limit of vanishing magnetic field our solution reduces to the supersymmetric background constructed in [15].

In section 3 of this paper we introduce a probe flavor brane to the supersymmetric background obtained in [15]. We first consider the case of supersymmetric embeddings and perform a holographic regularization of the probe brane action. Our findings enable us to propose an AdS/CFT dictionary applicable at the finite UV cut off of the theory. Next we consider D7-brane embeddings with fixed worldvolume gauge field. On the field theory side this corresponds to a constant external magnetic field coupled only to the fundamental degrees of freedom introduced by the probe brane. Using the proposed AdS/CFT dictionary we obtain numerical plot of the fundamental condensate versus the bare mass parameter and explore the effect that the presence of backreacted massless flavors have on the effect of magnetic catalysis of mass generation. Our findings suggest that the effect is to make the magnetic catalysis less efficient.

In Section 4 we generalize the study of Section 3 for an external magnetic field coupling to both the probe and the backreacted fundamental flavors. To this end, we consider a probe D7-brane in the non-supersymmetric background constructed in Section 2. We identify the value of the non-trivial B -field at the finite UV cut off as the value of the external magnetic field in the corresponding field theory. Our study of the classical embeddings of the probe brane suggest that for sufficiently low values of the perturbative parameter $\epsilon_* < \epsilon_{cr}$ the stable phase of the theory exhibit dynamical mass generation. However for sufficiently large values of $\epsilon_* = \epsilon_{cr}$ the theory is unstable. This instability is manifest as a diverging slope of the plot of the parameter of the IR separation (related to the constituent mass of the probe fundamental flavors) versus the parameter ϵ_* . We find further evidence for this instability by studying the meson spectrum of the theory and identifying appropriate tachyonic modes. We interpret the instability of the probe as reflecting an instability of the supergravity background.

In the Conclusion section of the paper we discuss briefly our present results and their possible extensions.

2. Constructing the background

The main goal we want to address with the gravity background of the following subsection is the study of the phenomenon of mass generation in magnetic catalysis. The field theories we are interested in are realized on the intersection between a set of N_c *color* D3-branes and a set of N_f , homogeneously smeared, *flavor* D7-branes. This is mainly the construction that was studied in [12] and in order to accommodate the phenomenon of mass generation we will impose an additional coupling between the fundamental fields and an external magnetic field.

The *color* D3-branes are placed at the tip of a Calabi-Yau (CY) cone over a Sasaki-Einstein manifold X_5 , where the latter can be expressed as a $U(1)$ fiber bundle over a four dimensional Kähler-Einstein base (KE). In the absence of flavor branes the *color* ones source a background whose near horizon

limit is the $AdS_5 \times X_5$ and the dual gauge theories are superconformal quivers.⁵

The *flavor* D7-branes introduce fundamental matter in the dual field theory. They extend along the radial direction of the background, wrap a submanifold X_3 of X_5 and at the same time smear homogeneously over the transverse space [18, 19]. The smeared distribution is taken in such a way that the isometries of the fibered Kähler-Einstein space are kept unbroken and allows to write an ansatz where all the unknown functions just depend on a single radial coordinate. The D7-brane embedding is described by a constant profile, implementing massless flavor fields in the dual gauge theory. As a general feature of all the D3-D7 setups, the dilaton runs and blows up at a certain radial distance, corresponding to a UV Landau pole in the dual gauge theory [15].

The presence of both kind of branes will deform the ten dimensional space-time, a product of a four dimensional Minkowski space with a six dimensional CY cone, through a (self dual) F_5 and an F_1 RR fields. The coupling of the *flavor* D7-branes with the external magnetic field will be realized by the simultaneous presence of a B_2 NS field and its electric dual C_2 RR field, along the gauge theory directions.

In the next subsection we will be precise about the mathematical expression of every one of the forms that we described above.

2.1 Ansatz

Our notation will follow closely [12, 14, 15]. The action for the of Type IIB supergravity coupled to N_f D7-branes, in the Einstein frame, is given by the following expression

$$S = S_{IIB} + S_{fl}, \quad (2.1)$$

where the terms of the S_{IIB} action are

$$S_{IIB} = \frac{1}{2\kappa_{10}^2} \int d^{10}x \sqrt{-g} \left[R - \frac{1}{2} \partial_M \Phi \partial^M \Phi - \frac{1}{2} e^{2\Phi} F_{(1)}^2 - \frac{1}{2} \frac{1}{3!} e^\Phi F_{(3)}^2 - \frac{1}{2} \frac{1}{5!} F_{(5)}^2 - \frac{1}{2} \frac{1}{3!} e^{-\Phi} H_{(3)}^2 \right] - \frac{1}{2\kappa_{10}^2} \int C_4 \wedge H_3 \wedge F_3, \quad (2.2)$$

and the action for the D7-branes takes the usual DBI+WZ form

$$S_{fl} = -T_7 \sum_{N_f} \left[\int d^8x e^\Phi \sqrt{-\det(\hat{G} + e^{-\Phi/2} \mathcal{F})} - \int_{D7} \hat{C}_q \wedge (e^{-\mathcal{F}})_{8-q} \right], \quad (2.3)$$

with $\mathcal{F} \equiv B + 2\pi\alpha' F$. In those expressions B denotes a non-constant magnetic field, F the world-volume gauge field and the hat refers to the pullback of the quantities, along the worldvolume directions of the D7-brane. The gravitational constant and D7-brane tension, in terms of string parameters, are

$$\frac{1}{2\kappa_{10}^2} = \frac{T_7}{g_s} = \frac{1}{(2\pi)^7 g_s^2 \alpha'^4}. \quad (2.4)$$

⁵For $X_5 = S^5$ the CY is the six dimensional Euclidean space and the dual field theory is $\mathcal{N} = 4$ SYM. For $X_5 = T^{1,1}$ the CY is the singular conifold and the dual theory is the Klebanov-Witten quiver [17].

The ansatz for the metric that we will adopt is inspired by [12] and has the following form

$$ds_{10}^2 = h^{-\frac{1}{2}} [-dt^2 + dx_1^2 + b(dx_2^2 + dx_3^2)] + h^{\frac{1}{2}} [b^2 S^8 F^2 d\sigma^2 + S^2 ds_{CP^2}^2 + F^2 (d\tau + A_{CP^2})^2], \quad (2.5)$$

where the CP^2 metric is given by

$$\begin{aligned} ds_{CP^2}^2 &= \frac{1}{4} d\chi^2 + \frac{1}{4} \cos^2 \frac{\chi}{2} (d\theta^2 + \sin^2 \theta d\varphi^2) + \frac{1}{4} \cos^2 \frac{\chi}{2} \sin^2 \frac{\chi}{2} (d\psi + \cos \theta d\varphi)^2 \quad \& \\ A_{CP^2} &= \frac{1}{2} \cos^2 \frac{\chi}{2} (d\psi + \cos \theta d\varphi). \end{aligned} \quad (2.6)$$

The range of the angles is $0 \leq (\chi, \theta) \leq \pi$, $0 \leq \varphi, \tau < 2\pi$, $0 \leq \psi < 4\pi$. The ansatz for the NS and the RR field strengths will be the following

$$B_2 = H dx^2 \wedge dx^3, \quad C_2 = J dt \wedge dx^1,$$

$$F_5 = Q_c (1 + *)\varepsilon(S^5), \quad F_1 = Q_f (d\tau + A_{CP^2}), \quad F_3 = dC_2 + B_2 \wedge F_1 \quad (2.7)$$

where $\varepsilon(S_5)$ is the volume element of the internal space and Q_c, Q_f are proportional to the number of colors and flavors

$$N_c = \frac{Q_c \text{Vol}(X_5)}{(2\pi)^4 g_s \alpha'^2} \quad \& \quad N_f = \frac{4 Q_f \text{Vol}(X_5)}{\text{Vol}(X_3) g_s}. \quad (2.8)$$

In our case $X_5 = S^5$ and the volume of the three sphere is $2\pi^2$. The fact that the flavors are massless is encoded in the independence of $F_{(1)}$ on σ , (see [10, 15]). All the functions that appear in the ansatz, h, b, S, F, Φ, J & H , depend on the radial variable σ . In the convention we follow, S & F have dimensions of length, b, h, J & H are dimensionless and σ has dimension length^{-4} . The ansatz for the F_3 RR field strength is determined by the ansatz for F_1 (see Appendix A for more details). Finally the function b in the ansatz for the metric reflects the breaking the of $SO(1, 3)$ Lorentz symmetry down to $SO(1, 1) \times SO(2)$.

The equations of motion and Bianchi identities following from (2.1) will be provided in full detail in Appendix A.

2.2 Effective action and the equations of motion

Since all the functions that participate in the ansatz for the solution, (2.5) & (2.7), depend only on σ , it is feasible to describe the system in terms of a one-dimensional effective action. In order to achieve that we insert all the ingredients of the ansatz in (2.1) and integrate out all the variables except σ arriving to

$$S_{eff} = \frac{\pi^3 V_{1,3}}{2\kappa_{10}^2} \int \mathcal{L}_{1d} d\sigma \quad (2.9)$$

where $V_{1,3}$ is the (infinite) volume of the Minkowski space and \mathcal{L}_{1d} is given by the following expression

$$\begin{aligned} \mathcal{L}_{1d} = & -\frac{1}{2} \left(\frac{h'}{h} \right)^2 + 12 \left(\frac{S'}{S} \right)^2 + 8 \frac{F' S'}{F S} + 24 b^2 F^2 S^6 - 4 b^2 F^4 S^4 \\ & + \frac{b'}{b} \left(\frac{h'}{h} + 8 \frac{S'}{S} + 2 \frac{F'}{F} \right) + \frac{1}{2} \left(\frac{b'}{b} \right)^2 - \frac{b^2 Q_c^2}{2 h^2} - \frac{1}{2} Q_f^2 b^2 e^{2\Phi} S^8 \left(1 + \frac{e^{-\Phi} H^2 h}{b^2} \right) \\ & - 4 Q_f b^2 e^\Phi F^2 S^6 \sqrt{1 + \frac{e^{-\Phi} H^2 h}{b^2}} - \frac{1}{2} \Phi'^2 - \frac{1}{2} \frac{e^{-\Phi} H'^2 h}{b^2} \left(1 - \frac{e^{2\Phi} J'^2 b^2}{H'^2} \right) - Q_c H J'. \end{aligned} \quad (2.10)$$

Producing (2.10) we have not made use of the WZ term, since it does not depend on the metric or the dilaton. Its effect has been taken into account through the expression for $F_{(1)}$ (see [15, 12]). The precise expression of the WZ term is needed in producing the equations of motion explicitly from (2.1) and it is this point that the smearing procedure enters the field and imposes the following replacement

$$\sum_{N_f} \int_{\mathcal{M}_8} \dots \longrightarrow \int_{\mathcal{M}_{10}} \Omega \wedge \dots, \quad (2.11)$$

where Ω is a form orthogonal to the D7-branes and we call it *smearing form*. The mathematical formula for the *smearing form* is given through the Bianchi identity for $F_{(1)}$ and it is

$$dF_1 = -g_s \Omega_2. \quad (2.12)$$

We will provide more details on the smearing of the DBI part of the action in Appendix A, where we will present all the details about the equations of motion and Bianchi identities of (2.1). Since the potential J enters the effective action only through its derivative, it corresponds to a “constant of motion”. This new parameter is related to the value of the magnetic field close to the boundary through the equations of motion for F_3 , coming from the 10d supergravity. We will fix this constant of motion in the following way

$$\frac{\partial \mathcal{L}_{1d}}{\partial J'} \equiv -Q_c H_* \quad \Rightarrow \quad J' = \frac{e^{-\Phi} Q_c}{h} (H - H_*). \quad (2.13)$$

The next step is to use equation (2.13) to eliminate J' , in favor of H_* , from (2.10) after performing the following Legendre transformation

$$\tilde{\mathcal{L}}_{1d} = L_{1d} - \frac{\delta L_{1d}}{\delta J'} J' \Big|_{J' \equiv J'(H_*)}. \quad (2.14)$$

The Euler-Lagrange equations will be calculated from the new, transformed, action (2.14). Defining the following auxiliary (dimensionless) expressions

$$\beta_1 \equiv \sqrt{1 + \frac{e^{-\Phi} H^2 h}{b^2}}, \quad \beta_2 \equiv 1 + \frac{e^{2\Phi} J'^2 b^2}{H'^2} \quad \& \quad \beta_3 \equiv 1 + \frac{e^{-2\Phi} H'^2 \beta_2}{Q_f^2 H^2 b^2 S^8} \quad (2.15)$$

we can write the equations of motion in the following compact way

$$\partial_\sigma^2(\log b) = -\frac{4Q_f H^2 h S^6 F^2}{\beta_1} - e^\Phi H^2 Q_f^2 h S^8 \beta_3 \quad (2.16)$$

$$\partial_\sigma^2(\log h) = -Q_c^2 \frac{b^2}{h^2} - \frac{2Q_f H^2 h S^6 F^2}{\beta_1} - \frac{1}{2} e^\Phi H^2 Q_f^2 h S^8 \beta_3 + (1 - \beta_2) \frac{e^{-\Phi} h H'^2}{b^2} \quad (2.17)$$

$$\partial_\sigma^2(\log S) = -2b^2 F^4 S^4 + 6b^2 F^2 S^6 - \frac{Q_f e^\Phi b^2 F^2 S^6}{\beta_1} + \frac{1}{4} e^\Phi H^2 Q_f^2 h S^8 \beta_3 \quad (2.18)$$

$$\partial_\sigma^2(\log F) = 4b^2 F^4 S^4 - \frac{1}{4} (1 + \beta_1^2) Q_f^2 e^{2\Phi} b^2 S^8 + \frac{Q_f H^2 h S^6 F^2}{\beta_1} + \frac{1}{4} \frac{e^{-\Phi} h H'^2 \beta_2}{b^2} \quad (2.19)$$

$$\partial_\sigma^2 \Phi = \frac{1}{2} (1 + \beta_1^2) \left[Q_f^2 e^{2\Phi} b^2 S^8 + \frac{4Q_f b^2 e^\Phi S^6 F^2}{\beta_1} \right] - \frac{1}{2} \frac{e^{-\Phi} h H'^2 \beta_2}{b^2} \quad (2.20)$$

$$\partial_\sigma \left[\frac{e^{-\Phi} h H'}{b^2} \right] = e^\Phi Q_f^2 H h S^8 + Q_c J' + \frac{4Q_f H h S^6 F^2}{\beta_1}. \quad (2.21)$$

It is straightforward to check that the above set of equations, together with (2.13), solve the full set of Einstein equations, provided the following “zero-energy” constraint is also satisfied

$$\begin{aligned} 0 = & -\frac{1}{2} \left(\frac{h'}{h} \right)^2 + 12 \left(\frac{S'}{S} \right)^2 + 8 \frac{F' S'}{F S} - 24 b^2 F^2 S^6 + 4 b^2 F^4 S^4 \\ & + \frac{b'}{b} \left(\frac{h'}{h} + 8 \frac{S'}{S} + 2 \frac{F'}{F} \right) + \frac{1}{2} \left(\frac{b'}{b} \right)^2 + \frac{b^2 Q_c^2}{2h^2} + \frac{1}{2} Q_f^2 b^2 e^{2\Phi} S^8 \beta_1^2 \\ & + 4 Q_f b^2 e^\Phi F^2 S^6 \beta_1 - \frac{1}{2} \Phi'^2 - \frac{1}{2} \frac{e^{-\Phi} h H'^2 \beta_2}{b^2} + \frac{1}{2} e^\Phi h J'^2. \end{aligned} \quad (2.22)$$

This constraint can be thought of as the $\sigma\sigma$ component of the Einstein equations. Differentiating (2.22) and using (2.13) & (2.16)–(2.21) we get zero, meaning that the system is not overdetermined.

2.3 Perturbative solution

The system (2.13) & (2.16)–(2.21) allows for a perturbative solution along the lines of [14]. There, the dimensionless parameter ϵ_* , which is connected to the position that the dilaton blows up, was introduced and subsequently used as an expansion parameter. In order for the solution to be valid on a large energy scale this parameter has to be a small number and in principle the smaller the value of the number the larger the range of the energy scale. After defining λ_* as the 't Hooft coupling at the energy scale r_* the parameter ϵ_* is expressed in terms of the physical quantities as

$$\epsilon_* = Q_f e^{\Phi_*} = \frac{\text{Vol}(X_3)}{16\pi \text{Vol}(X_5)} \lambda_* \frac{N_f}{N_c}, \quad (2.23)$$

and particularly for our case that $X_5 = S^5$ we have $\epsilon_* = \frac{1}{8\pi^2} \lambda_* \frac{N_f}{N_c}$. The parameter ϵ_* can be thought of as a flavor-loop counting parameter in the dual field theory.

Obtaining a perturbative solution, in terms of ϵ_* of the system (2.13) & (2.16)–(2.21), we need to impose the following two requirements to fix the constants of integration in the order by order expansion of the solution. The first one is that the geometries should coincide with the extremal ones in the absence of the magnetic field and the second is that the functions F, S & Φ should correspond to the expressions given in [14], at the energy scale $r = r_*$. We will redefine the radial variable σ in such a way that the warp factor keeps the standard *AdS* form

$$h = \frac{R^4}{r^4} \quad \& \quad R^4 \equiv \frac{1}{4} Q_c \quad (2.24)$$

therefore to first order in ϵ_* we have the following expression

$$\begin{aligned} \sigma = & \frac{1}{4r^4} + \epsilon_* \left[-\frac{1}{72r^4} \left[\frac{\alpha_r}{\alpha_r^2 - 1} - \frac{r^4}{r_*^4} \frac{\alpha_{r_*}}{\alpha_{r_*}^2 - 1} \right] + \frac{1}{96r^4} \left[\alpha_r (\alpha_r^2 - 1) - \frac{r^4}{r_*^4} \alpha_{r_*} (\alpha_{r_*}^2 - 1) \right] \right. \\ & - \frac{1}{192r^4} \left[(\alpha_r^2 - 1)^2 \log \left[\frac{\alpha_r + 1}{\alpha_r - 1} \right] - \frac{r^4}{r_*^4} (\alpha_{r_*}^2 - 1)^2 \log \left[\frac{\alpha_{r_*} + 1}{\alpha_{r_*} - 1} \right] \right] - \frac{17}{144r^4} (\alpha_r - \alpha_{r_*}) \\ & \left. - \frac{1}{16r^4} \left[(\alpha_r^2 - 1) \log \left[\frac{\alpha_r + 1}{\alpha_r - 1} \right] - (\alpha_{r_*}^2 - 1) \log \left[\frac{\alpha_{r_*} + 1}{\alpha_{r_*} - 1} \right] \right] + \frac{\alpha_{r_*}}{144r^4} \left(1 - \frac{r^4}{r_*^4} \right) \right], \quad (2.25) \end{aligned}$$

where another set of auxiliary dimensionless functions are in order

$$\alpha_r \equiv \sqrt{1 + \frac{e^{-\Phi_*} H_*^2 Q_c}{4r^4}} \quad \& \quad \alpha_{r_*} \equiv \sqrt{1 + \frac{e^{-\Phi_*} H_*^2 Q_c}{4r_*^4}}. \quad (2.26)$$

Having (2.25) to transform the solution of the system (2.13) & (2.16)–(2.21) from the one holographic

coordinate to the other we arrive to the following expressions for Φ , H , J' and b

$$\Phi = \Phi_* - \frac{\epsilon_*}{2} \left[\alpha_r - \alpha_{r_*} - \frac{1}{2} \log \left[\frac{(\alpha_r + 1)(\alpha_{r_*} - 1)}{(\alpha_r - 1)(\alpha_{r_*} + 1)} \right] \right] \quad (2.27)$$

$$H = H_* \left[1 - \frac{\epsilon_*}{8} \left[\alpha_r \frac{\alpha_r^2 + 1}{\alpha_r^2 - 1} - \alpha_{r_*} \frac{\alpha_{r_*}^2 + 1}{\alpha_{r_*}^2 - 1} \frac{r^4}{r_*^4} - \frac{\alpha_r^2 - 1}{2} \log \left[\frac{\alpha_r + 1}{\alpha_r - 1} \right] \right. \right. \\ \left. \left. + \frac{\alpha_{r_*}^2 - 1}{2} \log \left[\frac{\alpha_{r_*} + 1}{\alpha_{r_*} - 1} \right] \frac{r^4}{r_*^4} \right] \right] \quad (2.28)$$

$$J' = \epsilon_* \frac{e^{-\Phi_*} H_*}{2r} \left[\alpha_r \frac{\alpha_r^2 + 1}{\alpha_r^2 - 1} - \alpha_{r_*} \frac{\alpha_{r_*}^2 + 1}{\alpha_{r_*}^2 - 1} \frac{r^4}{r_*^4} - \frac{\alpha_r^2 - 1}{2} \log \left[\frac{\alpha_r + 1}{\alpha_r - 1} \right] \right. \\ \left. + \frac{\alpha_{r_*}^2 - 1}{2} \log \left[\frac{\alpha_{r_*} + 1}{\alpha_{r_*} - 1} \right] \frac{r^8}{r_*^8} \right] \quad (2.29)$$

$$b = 1 + \frac{\epsilon_*}{2} \left[\alpha_r - \alpha_{r_*} + \frac{1}{2} (\alpha_r^2 - 1) \log \left[\frac{\alpha_r + 1}{\alpha_r - 1} \right] - \frac{1}{2} (\alpha_{r_*}^2 - 1) \log \left[\frac{\alpha_{r_*} + 1}{\alpha_{r_*} - 1} \right] \right]. \quad (2.30)$$

Integrating (2.22) we have for F & S

$$F + 4S = 5r + \frac{\epsilon_*}{2} \left[-\frac{r}{16} \left[\alpha_r (\alpha_r^2 - 1) - \frac{r^4}{r_*^4} \alpha_{r_*} (\alpha_{r_*}^2 - 1) \right] + \frac{r r^4}{9 r_*^4} \right. \\ \left. + \frac{r}{8} \left[\alpha_r - \frac{r^4}{r_*^4} \alpha_{r_*} \right] + \frac{r}{4} \left[\frac{\alpha_r}{\alpha_r^2 - 1} - \frac{r^4}{r_*^4} \frac{\alpha_{r_*}}{\alpha_{r_*}^2 - 1} \right] \right. \\ \left. + \frac{r}{32} \left[(\alpha_r^2 - 1)^2 \log \left[\frac{\alpha_r + 1}{\alpha_r - 1} \right] - \frac{r^4}{r_*^4} (\alpha_{r_*}^2 - 1)^2 \log \left[\frac{\alpha_{r_*} + 1}{\alpha_{r_*} - 1} \right] \right] \right] \quad (2.31)$$

while decoupling (2.18) & (2.19)

$$F - S = -\frac{\epsilon_*}{12} \left[\frac{r}{4} \left[\alpha_r (\alpha_r^2 - 1) - \frac{r^2}{r_*^2} \alpha_{r_*} (\alpha_{r_*}^2 - 1) \right] + r \frac{r^2}{r_*^2} - \frac{r}{4} (\alpha_r^2 - 1)^{3/2} \left(1 - \frac{r^8}{r_*^8} \right) \right. \\ \left. + \frac{5r}{8} \left[\alpha_r - \frac{r^2}{r_*^2} \alpha_{r_*} \right] + \frac{3}{8} \frac{r}{\sqrt{\alpha_r^2 - 1}} \log \left[\frac{\alpha_r + \sqrt{\alpha_r^2 - 1}}{\alpha_{r_*} + \sqrt{\alpha_{r_*}^2 - 1}} \right] \right]. \quad (2.32)$$

2.4 Validity of the perturbative solution

The perturbative solution we present in the preceding section needs to be supplemented with a hierarchy of scales. In terms of the radial coordinate r (or σ) our solution has two pathological regions that we will describe in this section both qualitatively & quantitatively.

As explained in the introduction, the background we have constructed consists of a sea of massless flavors. This means that the flavor branes are stretched down to the bottom of the geometry and the charge density is highly peaked at $r = 0$. This is the reason behind the curvature singularity that appears in the origin.⁶ Another way to understand this pathology is through the restoration of the $U(N_f)$ symmetry in the deep IR and the subsequent increase of the effective string coupling in such a way that the smearing approach breaks down. Careful choice of the integration constants when obtaining the perturbative solution together with the presence of the magnetic field, produce a less severe IR singularity but by no means cure it.

A crucial point is that due to the infrared divergency of the background the perturbative solution presented in equations (2.25)–(2.32) is not valid below certain radial distance above the origin. In particular the Jacobean $\left| \frac{\partial \sigma}{\partial r} \right|$ is vanishing at some $r_{IR}(\epsilon_*)$. As one may expect if we increase the number of backreacted flavors the value for the radius $r_{IR}(\epsilon)$ increases. One can imagine that higher order corrections in ϵ_* could reduce the value $r_{IR}(\epsilon)$, however the intrinsic infrared divergency of the background at the origin suggests that r_{IR} remains non-vanishing in any perturbative solution. In Sections 3 and 4 we will use this radius as a parameter characterizing the infrared applicability of our probe-brane analysis.

There are two ways of either avoiding or hiding the infrared singularity. The first one is to pull the flavor branes away from the origin, while keeping the radial symmetry, by introducing massive flavors. Then the distance between the color and the flavor branes is interpreted as a mass for the fundamentals. The second possibility is the addition of temperature to the background, which has effect of hiding the singularity behind the horizon, see [12].

A common characteristic of all the unquenched holographic backgrounds constructed so far is the appearance of a point in the deep UV that the dilaton diverges. This behavior is a signal for a Landau pole in the dual gauge theory.⁷ The perturbative solution we constructed in the previous section is valid until $r = r_*$, where r_* denotes an (arbitrary) UV cutoff scale $\frac{r_*}{R^2} \sim \Lambda_{UV}$, well below the energy scale of the Landau pole. Additionally the energy scale of r_* should be well above the IR scale, in order for the UV completion to have only negligible effects in the IR physics. The main characteristic of this scale is that the UV details of the theory do not affect the IR physical predictions. This feature is reflected by the independence of all physical quantities (up to suppressed contributions) on the position of r_* but only on IR parameters. The quantitative outcome of the above analysis is that $\epsilon_* \ll 1$, [12, 14], and as we increase the number of flavors the *effective physical region* for the solution between the IR & UV energy scales decreases.

3. Probing the supersymmetric background

In this section we introduce a probe D7-brane to the supersymmetric background of [15], which is the limit of vanishing magnetic field for the perturbative supergravity background constructed above. We consider both supersymmetric and non supersymmetric embeddings. The latter have a

⁶A very nice visualization of this construction can be found in [8].

⁷The first counter example is the addition of flavor D6-branes to the ABJM [20], where the smeared unquenched supergravity solution has a *good* UV behavior.

fixed value of the $U(1)$ -gauge field strength along the coordinates x_2 and x_3 , namely $F_{23} = \text{const}$. On the field theory side this corresponds to an external magnetic field coupling only to the fundamental degrees of freedom introduced by the probe D7-brane. We will contrast those results to the ones of Section 4, where the external magnetic field couples to all the fundamental degrees of freedom. Let us begin by studying the properties of the supersymmetric embeddings.

3.1 Holographic renormalization

In this subsection we propose a holographic renormalization scheme similar to the one reported in [21] for asymptotically AdS gravitational backgrounds. Our goal is to come up with a prescription to calculate vacuum expectation values (like the fundamental condensate) for the supergravity background of [15], which suffers from UV divergencies. In the limit of vanishing magnetic field the first order perturbative solution is given by [12]

$$\begin{aligned} \Phi &= \Phi_* + \epsilon_* \log \frac{r}{r_*} + \mathcal{O}(\epsilon_*^2), \quad b = 0, \quad h = \frac{R^4}{r^2} \\ F_0 &= r \left[1 - \epsilon_* \frac{1}{24} \left(1 + \frac{1}{3} \frac{r^4}{r_*^4} \right) \right] + \mathcal{O}(\epsilon_*^2) \quad \& \quad S_0 = r \left[1 + \epsilon_* \frac{1}{24} \left(1 - \frac{1}{3} \frac{r^4}{r_*^4} \right) \right] + \mathcal{O}(\epsilon_*^2). \end{aligned} \quad (3.1)$$

The lagrangian of the D7-brane probe is given by

$$-\frac{\mathcal{L}}{\mathcal{N}} = \frac{e^\Phi}{8r^5} S_0^6 F_0^2 \cos^3 \frac{\chi}{2} \left(\cos^2 \frac{\chi}{2} + \frac{S_0^2}{F_0^2} \sin^2 \frac{\chi}{2} \right)^{\frac{1}{2}} \left(1 + \frac{r^{10} \chi'^2}{4S_0^6 F_0^2} \right)^{\frac{1}{2}} + \frac{\epsilon_* e^{2\Phi - \Phi_*}}{32r^5} S_0^8 \cos^4 \frac{\chi}{2}, \quad (3.2)$$

where $\mathcal{N} \equiv 8 T_7 \text{Vol}(S^3) V_{1,3}$ with $V_{1,3}$ the volume spanned by (t, x^i) and $\text{Vol}(S^3) = 2\pi^2$ the volume of the unit S^3 wrapped by the probe brane. In the next step we expand the classical embedding around ϵ_* according to $\chi = \chi_0(r) + \epsilon_* \chi_1(r)$ and solve perturbatively the EOM obtained from (3.2). The zeroth order lagrangian is given by

$$-\frac{\mathcal{L}_0}{\mathcal{N}} = \frac{1}{8} e^{\Phi_*} r^3 \cos^3 \frac{\chi_0(r)}{2} \left(1 + \frac{r^2}{4} \chi_0'(r)^2 \right)^{1/2}, \quad (3.3)$$

which is just the lagrangian for a D7-brane probe in pure $\text{AdS}_5 \times S^5$ space time analyzed in [9] (in slightly different coordinates). The solution for a supersymmetric embedding corresponding to flavor with bare mass $m/(2\pi\alpha')$ is given by

$$\chi_0(r) = 2 \arcsin \frac{m}{r}. \quad (3.4)$$

The solution for $\chi_1(r)$ corresponding to the first order correction to (3.4) is

$$\chi_1(r) = \frac{m \left[r^4 - m^4 + 12 r_*^4 \log \left(\frac{m}{r} \right) \right]}{36 r_*^4 \sqrt{r^2 - m^2}}. \quad (3.5)$$

In the next step we substitute (3.4) and (3.5) in the lagrangian (3.2), obtain the “on-shell” lagrangian \mathcal{L}_{cl} to first order in ϵ_*

$$-\frac{\mathcal{L}_{cl}}{\mathcal{N}} = \frac{1}{8}e^{\Phi_*}r(r^2 - m^2) + \frac{\epsilon_* e^{\Phi_*}}{288 r r_*^4} \left[-12 m^2 r^2 r_*^4 \log\left(\frac{m}{r}\right) \right. \\ \left. - (r^2 - m^2) \left[m^4 r^2 + 4 r^6 - 15 r^2 r_*^4 + m^2 (r^4 + 3r_*^4) - 36 r^2 r_*^4 \log\left(\frac{r}{r_*}\right) \right] \right] \quad (3.6)$$

and then integrate it from m to r_* . Note that since $\chi_1(m) = 0$ the classical embedding of the D7-brane, to first order, closes at $r = m$ above the origin. It is convenient to define

$$S_{cl} = \int_m^{r_*} dr \mathcal{L}_{cl} = S_{cl}^{(0)} + \epsilon_* S_{cl}^{(1)} + \mathcal{O}(\epsilon_*^2), \quad (3.7)$$

and after that expand in powers r_*

$$-\frac{S_{cl}^{(0)}}{\mathcal{N}e^{\Phi_*}} = \frac{1}{32}(r_*^2 - m^2)^2 = \frac{r_*^4}{32} - \frac{r_*^2 m^2}{16} + \frac{m^4}{32}, \quad (3.8)$$

$$-\frac{S_{cl}^{(1)}}{\mathcal{N}e^{\Phi_*}} = \frac{r_*^4}{288} - \frac{r_*^2 m^2}{576} \left[5 + 12 \log\left(\frac{m}{r_*}\right) \right] + \frac{m^4}{192} \left[1 + 4 \log\left(\frac{m}{r_*}\right) \right] + \mathcal{O}\left(\frac{1}{r_*^2}\right). \quad (3.9)$$

The divergent and finite terms can be canceled [21] by the addition of the following counter terms at $r = r_*$

$$L_1 = \#_1 e^{\Phi} \sqrt{-\gamma}, \quad L_2 = \#_2 e^{\Phi} \sqrt{-\gamma} \chi^2 \quad \& \quad L_f = \#_f e^{\Phi} \sqrt{-\gamma} \chi^4, \quad (3.10)$$

where $\#_1, \#_2$ and $\#_f$ are appropriately chosen coefficients and γ is the determinant of the induced metric on the $r = \text{const}$ slice. Note that we have integrated along all the compact directions (their contribution is included in \mathcal{N}) and we have added a factor of e^{Φ} to all the counter terms. To first order in ϵ_* we have the following divergent and finite contributions from the counter terms

$$\frac{L_1}{\#_1 e^{\Phi_*}} = \frac{r_*^4}{R^4}, \quad (3.11)$$

$$\frac{L_2}{\#_2 e^{\Phi_*}} = \frac{4r_*^2 m^2}{R^4} + \frac{4m^4}{3R^4} + \epsilon_* \frac{m^2}{9R^4} \left(r_*^2 + \frac{2}{3} m^2 \right) \left[1 + 12 \log\left(\frac{m}{r_*}\right) \right], \quad (3.12)$$

$$\frac{L_f}{\#_f e^{\Phi_*}} = \frac{16m^4}{R^4} + \epsilon_* \frac{8m^4}{9R^4} \left[1 + 12 \log\left(\frac{m}{r_*}\right) \right]. \quad (3.13)$$

One can check that the following set of coefficients

$$\#_1 = \mathcal{N} \frac{R^4}{32} \left(1 + \frac{1}{9} \epsilon_* \right), \quad (3.14)$$

$$\#_2 = -\mathcal{N} \frac{R^4}{64} \left(1 + \frac{1}{9} \epsilon_* \right), \quad (3.15)$$

$$\#_f = \mathcal{N} \frac{5R^4}{1536} \left(1 + \frac{1}{9} \epsilon_* \right) \quad (3.16)$$

cancels all the divergent and finite terms in the first order of the “on-shell” action $S_{cl}^{(0)} + \epsilon_* S_{cl}^{(1)}$.

An interesting observation coming from (3.14), (3.15) and (3.16) is that the coefficient of all the counter terms has the same ϵ_* dependence, namely $(1 + \epsilon_*/9)$. In fact one can check that this remains true also for the second order corrections, suggesting that resummation is possible. Indeed, it turns out that if one considers the non-perturbative form of the solution the ϵ_* dependence of the “on-shell” action factorizes. Let us briefly sketch the derivation. The supersymmetric background is determined by the following set of first order differential equations [12]

$$S = \alpha'^{\frac{1}{2}} e^\rho \left[1 + \epsilon_* \left(\frac{1}{6} + \rho_* - \rho \right) \right]^{\frac{1}{6}}, \quad (3.17)$$

$$F = \alpha'^{\frac{1}{2}} e^\rho [1 + \epsilon_* (\rho_* - \rho)]^{\frac{1}{2}} \left[1 + \epsilon_* \left(\frac{1}{6} + \rho_* - \rho \right) \right]^{-\frac{1}{3}}, \quad (3.18)$$

$$\Phi = \Phi_* - \log [1 + \epsilon_* (\rho_* - \rho)], \quad (3.19)$$

$$\frac{dh}{d\rho} = -Q_c \alpha'^{-2} e^{-4\rho} \left[1 + \epsilon_* \left(\frac{1}{6} + \rho_* - \rho \right) \right]^{-\frac{2}{3}}, \quad (3.20)$$

where a new radial coordinate ρ has been introduced. The relation between r and the new radial variable ρ can be obtained as an expansion in powers series of ϵ_* and to first order is given by [12]

$$r = \alpha'^{\frac{1}{2}} e^\rho \left[1 + \frac{\epsilon_*}{72} [e^{4\rho - 4\rho_*} - 1 + 12(\rho_* - \rho)] \right] + \mathcal{O}(\epsilon_*^2). \quad (3.21)$$

Note that for $\epsilon_* = 0$ one has simply $r = \alpha'^{\frac{1}{2}} e^\rho$, while this relation also holds at $r = r_*$ for arbitrary ϵ_* . Therefore at $\epsilon_* = 0$ the supersymmetric embedding $\chi(\rho)$ corresponding to $\chi_0(r)$ from (3.4) is

$$\chi(\rho) \equiv 2 \arcsin \frac{e^{\rho q}}{e^\rho}. \quad (3.22)$$

The parameter $e^{\rho q}$ is related to the bare mass of the fundamental degrees of freedom introduced by the probe. It turns out that the supersymmetric embedding at finite ϵ_* is still given by equation

(3.22)⁸, see [12]. The next step is to evaluate the “on-shell” action S_{cl} and for this we note the zeroth order term in (3.8) which suggests the following $-S_{cl}^{(0)}/(\mathcal{N}\alpha'^2) = e^{\Phi_*}(e^{2\rho_*} - e^{2\rho_q})^2/32$. The classical action to all orders in ϵ_* has the following expression⁹

$$-\frac{S_{cl}(\epsilon_*)}{\mathcal{N}\alpha'^2} = \frac{e^{\Phi_*}}{32} \left(1 + \frac{\epsilon_*}{6}\right)^{\frac{2}{3}} (e^{2\rho_*} - e^{2\rho_q})^2. \quad (3.23)$$

Remarkably the ϵ_* dependence of the “on-shell” action factorizes when it is written in the radial coordinate ρ . Furthermore, since at $r = r_*$ the relation between the two radial coordinates is $r_* = \alpha'^{\frac{1}{2}}e^{\rho_*}$ the ϵ_* dependence of the “on-shell” action remains unchanged if one defines $m_0 = \alpha'^{\frac{1}{2}}e^{\rho_q} = m + O(\epsilon_*)$ as a bare mass parameter. This suggests that to all orders in ϵ_* the counter terms are given by equation (3.10) with the following coefficients $\#_1, \#_2, \#_3$

$$\#_1 = \mathcal{N} \frac{R^4}{32} \left(1 + \frac{1}{6}\epsilon_*\right)^{\frac{2}{3}}, \quad (3.24)$$

$$\#_2 = -\mathcal{N} \frac{R^4}{64} \left(1 + \frac{1}{6}\epsilon_*\right)^{\frac{2}{3}}, \quad (3.25)$$

$$\#_f = \mathcal{N} \frac{5R^4}{1536} \left(1 + \frac{1}{6}\epsilon_*\right)^{\frac{2}{3}}. \quad (3.26)$$

The above considerations suggest that one can consistently regularize the “on-shell” action of the probe D7-brane provided one keeps the parameter ϵ_* sufficiently small to ensure that the finite cut off $r_* = \alpha'^{\frac{1}{2}}e^{\rho_*}$ is sufficiently far from the Landau pole of the theory and at the same time is sufficiently large so that terms of order $\mathcal{O}(e^{-\rho_*})$ can be ignored in calculating the regularized “on-shell” action. Therefore we propose that the usual AdS/CFT dictionary can be applied at $r = r_*$, namely one can expand

$$\sin \frac{\chi(r_*)}{2} = \frac{m_0}{r_*} + \frac{c}{r_*^3} + O\left(\frac{1}{r_*^5}\right) \quad (3.27)$$

and identify $m_0 = \alpha'^{\frac{1}{2}}e^{\rho_q}$ as the bare mass parameter and $c \propto \langle \bar{q}q \rangle$ as the fundamental condensate. Note that for the supersymmetric embedding of (3.22) we have $c = 0$ and thus the fundamental condensate vanish (as it should for supersymmetric theory). In the next subsection we will consider non-supersymmetric embeddings with fixed $U(1)$ gauge field strength $F_{23} = \text{const}$ and apply the proposed dictionary to study the fundamental condensate of the theory.

3.2 D7-brane probe with fixed $U(1)$ -gauge field.

In this subsection we introduce a D7-brane probe with fixed $U(1)$ gauge field strength $F_{23} = H_0/2\pi\alpha'$. On the field theory side this corresponds to coupling the $\mathcal{N} = 2$ hypermultiplet with

⁸Note that equation (3.21) suggests that $m \equiv r(\rho_q) = \alpha'^{\frac{1}{2}}e^{\rho_q} + O(\epsilon)$.

⁹We refer the reader to the appendix of the paper for more details on this calculation.

a constant external magnetic field $H_0/2\pi\alpha'$ along the x_1 direction. The effective action of the probe brane in the Einstein frame is

$$\mathcal{S} = -T_7 \int d^8x e^\Phi \sqrt{-\det(\hat{g} + e^{-\Phi/2} B_2)} + T_7 \int P[C_{(8)}], \quad (3.28)$$

where $C_{(8)}$ is the background Ramond-Ramond form sourced by the smeared flavor branes. One can show that the effective lagrangian is

$$-\frac{\mathcal{L}}{\mathcal{N}} = \frac{1}{8} e^\Phi S^6 F^2 \cos^3 \frac{\chi}{2} \left(\cos^2 \frac{\chi}{2} + \frac{S^2}{F^2} \sin^2 \frac{\chi}{2} \right)^{1/2} \left(1 + \frac{\chi'^2}{4S^6 F^2} \right)^{1/2} (1 + e^{-\Phi} H_0^2 h)^{1/2} + \frac{Q_f}{32} e^{2\Phi} S^8 \cos^4 \frac{\chi}{2}, \quad (3.29)$$

where the functions F , S , Φ & h are given in equations (3.17)-(3.20). Note that in (3.20) the equation of motion for h is in an integral form but it can be obtained in terms of incomplete gamma functions. We refer the reader to the appendix for the technical details.

It turns out that for the numerical analysis it is convenient to define the following dimensionless quantities

$$\tilde{\rho} = \rho - \rho_m, \quad \tilde{r} = r/r_m, \quad \& \quad \rho_m \equiv \log \frac{r_m}{\sqrt{\alpha'}} \equiv \frac{1}{4} \log \frac{e^{-\Phi_*} Q_c H_0^2}{4\alpha'^2}. \quad (3.30)$$

Next we proceed by solving numerically the equation of motion for the classical embedding of the probe $\chi(\tilde{\rho})$ and expanding at $\tilde{\rho} = \tilde{\rho}_* = \log(\tilde{r}_*)$

$$\sin \frac{\chi(\tilde{r}_*)}{2} = \frac{\tilde{m}}{\tilde{r}_*} + \frac{\tilde{c}}{r_*^3} + \mathcal{O}\left(\frac{1}{\tilde{r}_*^5}\right) \quad \text{with} \quad \tilde{m} = m_0/r_m \quad \& \quad \tilde{c} = c/r_m^3; \quad (3.31)$$

where as we discussed above m_0 & c are related to the bare mass and the fundamental condensate of the $\mathcal{N} = 2$ hypermultiplet corresponding to the probe brane. Next we vary the parameter ϵ_* and generate plots of $-\tilde{c}$ versus \tilde{m} , which we present in figure 1.

The first plot corresponds to a very small value of ϵ_* , namely 10^{-3} . One may expect that for such a small value the qualitative and quantitative behavior of the system would be the same as for the case of pure $\text{AdS}_5 \times S^5$ space-time, studied in [3]. Indeed our results confirm that. The other plots in figure 2 correspond to $\epsilon_* = 0.25, 0.5, 0.75$. One can observe that qualitatively the theory has the same properties. For sufficiently low bare mass (strong magnetic field) there are multiple phases forming a spiral structure near the origin of the $-\tilde{c}$ versus \tilde{m} plane. Only the lowest positive ($\tilde{m} > 0$) branch of the spiral corresponds to a stable phase [22]. Furthermore at vanishing bare mass the theory has a non-vanishing negative condensate which spontaneously breaks a global $U(1)$ R-charge symmetry. As one can see the only effect of the backreaction is to lower the value of this condensate.

In figure 2 we have presented a plot of the symmetry breaking condensate (at vanishing bare mass) as a function of the parameter ϵ_* . We have normalized the plots in units of the condensate at

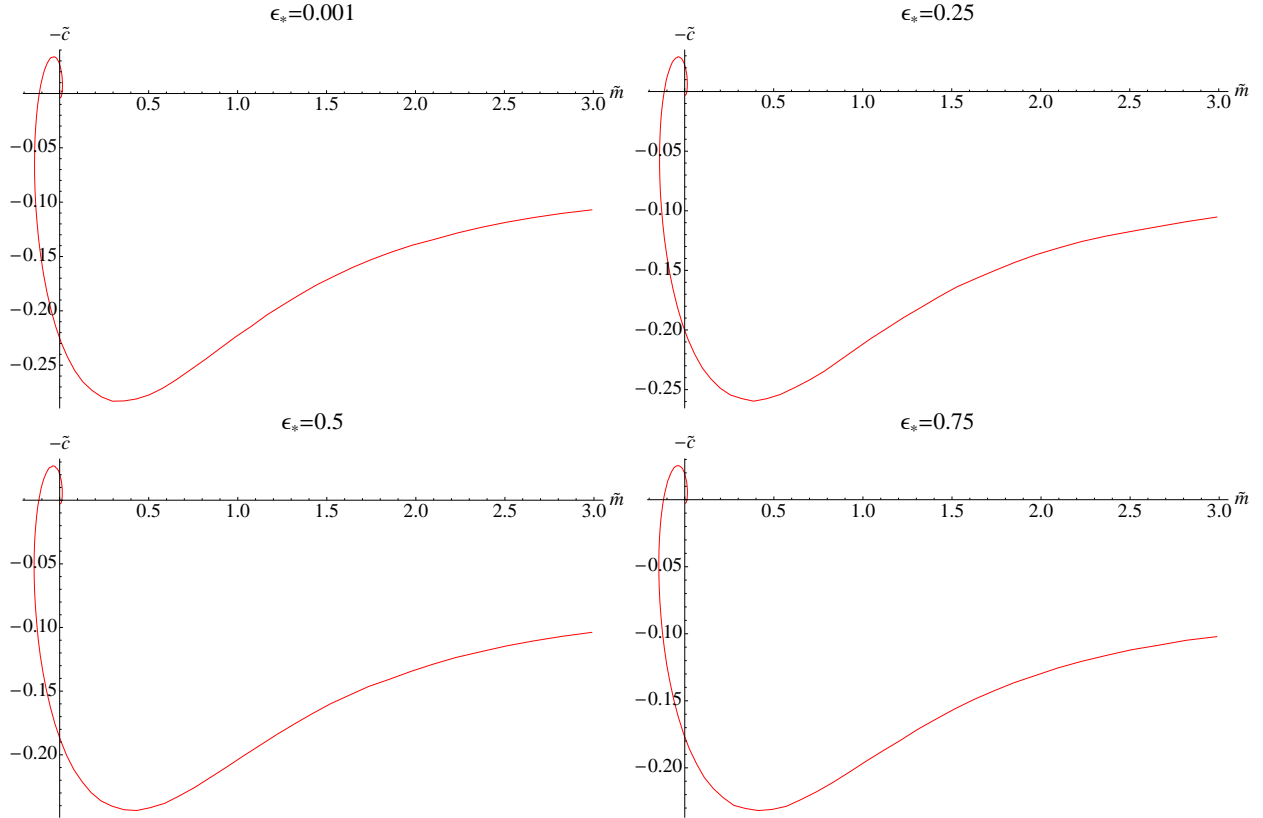


Figure 1: Plots of the parameter $-\tilde{c}$ (fundamental condensate) versus the parameter \tilde{m} (bare mass) for various values of the parameter ϵ_* . The shape of the plots remains unchanged.

vanishing ϵ_* . Note that one can vary ϵ_* either at fixed r_m (fixed magnetic field) or at fixed infrared separation $L_0 = r_{min}$ (the radial distance above the origin at which the S^3 wrapped by the probe brane shrinks). As one can see in both cases the fundamental condensate decreases as we increase ϵ_* . Note that in figure 2 we keep the value ϵ_* between zero and one, even if it is possible to extend this range. The reason behind this choice is the separation of scales, which keeps the finite cut off well below the Landau pole only in the limit $\epsilon_* \ll 1$.

4. Probing the fully backreacted background

In this section we introduce a probe D7-brane to the perturbative background obtained in section 2. On the field theory side this corresponds to an introduction of additional fundamental flavors. The fundamental fields couple to the background B -field, which on the field theory side corresponds to an external magnetic field. Therefore, in the limit of vanishing bare mass we expect to observe the phenomenon of magnetic catalysis of mass generation according to [3]. The novel feature of our set up is the presence of smeared backreacted flavors which number is controlled by the parameter ϵ_* . Our immediate goal is to study the effect of the presence of the sea of massless fundamental fields on the process of mass generation. Note that in this set up the external magnetic field couples to

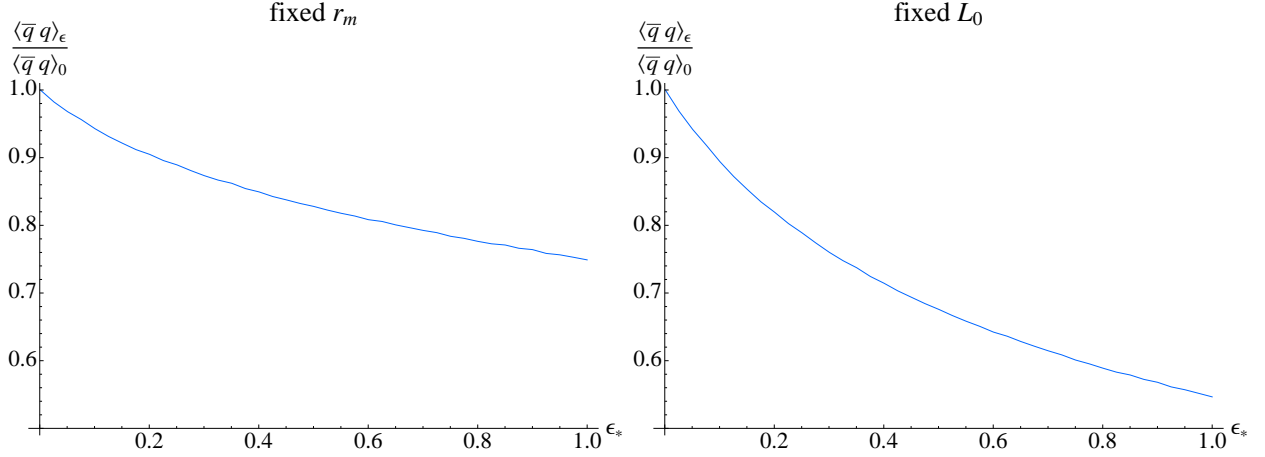


Figure 2: Plots of the dependence of the scaled fundamental condensate $\langle \bar{q}q \rangle_{\epsilon_*} / \langle \bar{q}q \rangle_0$ versus the small parameter ϵ_* . The left plot corresponds to varying ϵ_* at fixed r_m (fixed magnetic field) and the right plot corresponds to fixed infrared separation L_0 (fixed constituent mass).

the smeared massless fundamental flavors. This is to be contrasted to the case studied in section 3.2, when the external magnetic field couples only to the flavor fields introduced by the probe brane. Our investigation indicates a significant change in the physical properties of the system.

4.1 Classical embeddings

Let us begin by considering a probe D7-brane extended along the $t, x^i, \sigma, \theta, \psi, \phi$ coordinates and having a non trivial profile along the coordinate χ . The effective action of the probe in the Einstein frame is

$$\mathcal{S} = -T_7 \int d^8x e^\Phi \sqrt{-\det(\hat{g} + e^{-\Phi/2} B_2)} + T_7 \int P[C_{(8)} - B_{(2)} \wedge C_{(6)}], \quad (4.1)$$

where $C_{(8)}$ and $C_{(6)}$ are background Ramond-Ramond forms sourced by the smeared flavor branes. One can show that the effective lagrangian is

$$\begin{aligned} \mathcal{L}^{(0)} \propto & \frac{1}{8} e^\Phi b^2 S^6 F^2 \cos^3 \frac{\chi}{2} \left(\cos^2 \frac{\chi}{2} + \frac{S^2}{F^2} \sin^2 \frac{\chi}{2} \right)^{1/2} \left(1 + \frac{\chi'^2}{4b^2 S^6 F^2} \right)^{1/2} \left(1 + \frac{e^{-\Phi} H^2 h}{b^2} \right)^{1/2} \\ & + \frac{Q_f}{32} e^{2\Phi} b^2 S^8 \left(1 + \frac{e^{-\Phi} H^2 h}{b^2} \right) \cos^4 \frac{\chi}{2}. \end{aligned} \quad (4.2)$$

We find it convenient to introduce the radial variable r related to σ via (2.25). In order to obtain numerical solutions for the classical embedding, we define as usual the following dimensionless variable

$$\tilde{r} = \frac{r}{r_m}, \quad \text{with} \quad r_m \equiv \frac{e^{-\Phi_*} Q_c H_*^2}{4}. \quad (4.3)$$

It is convenient to write the dimensionless action in terms of the following auxiliary functions

$$\tilde{\mathcal{L}}^{(0)} = -f_1(\tilde{r}) \left(\cos^2 \frac{\chi}{2} + f_2(\tilde{r})^2 \sin^2 \frac{\chi}{2} \right)^{1/2} \sqrt{1 + f_3(\tilde{r})^2 \chi'^2} + f_4(\tilde{r}) \cos^4 \frac{\chi}{2}, \quad (4.4)$$

where

$$\begin{aligned}
f_1(\tilde{r}) &= \frac{1}{8} e^{\tilde{\Phi}} \tilde{b}^2 \tilde{S}^6 \tilde{F}^2 \left(1 + \frac{e^{-\tilde{\Phi}} \tilde{H}^2}{\tilde{r}^4 \tilde{b}^2} \right)^{\frac{1}{2}} \left| \frac{\partial \tilde{\sigma}}{\partial \tilde{r}} \right|, & f_2(\tilde{r}) &= \frac{\tilde{S}}{\tilde{F}}, \\
f_3(\tilde{r}) &= \left(2 \tilde{b} \tilde{S}^3 \tilde{F} \left| \frac{\partial \tilde{\sigma}}{\partial \tilde{r}} \right| \right)^{-1}, & f_4(\tilde{r}) &= \frac{\epsilon_*}{32} e^{2\tilde{\Phi}} \tilde{b}^2 \tilde{S}^8 \left(1 + \frac{e^{-\tilde{\Phi}} \tilde{H}^2}{\tilde{r}^4 \tilde{b}^2} \right) \left| \frac{\partial \tilde{\sigma}}{\partial \tilde{r}} \right|,
\end{aligned} \tag{4.5}$$

and $\tilde{\Phi}$, \tilde{b} , \tilde{S} , \tilde{F} , \tilde{H} , $\tilde{\sigma}$ are related to the functions defined in equations (2.25)-(2.32) via

$$\begin{aligned}
\tilde{\Phi}(\tilde{r}) &= \Phi(\tilde{r}r_m) - \Phi_*, & \tilde{b}(\tilde{r}) &= b(\tilde{r}r_m), & \tilde{S}(\tilde{r}) &= S(\tilde{r}r_m)/r_m, \\
\tilde{F} &= F(\tilde{r}r_m)/r_m, & \tilde{H}(\tilde{r}) &= H(\tilde{r}r_m)/H_*, & \tilde{\sigma}(\tilde{r}) &= \sigma(\tilde{r}r_m)r_m^4.
\end{aligned} \tag{4.6}$$

One can show that a smooth solution to the equations of motion derived from (4.4) valid near the point that the S^3 -sphere, wrapped by the probe brane, shrinks ($\chi(\tilde{r}_{min}) = \pi$) is

$$\chi(\tilde{r}) = \pi - \sqrt{a(\tilde{r} - \tilde{r}_{min})}, \quad a = \frac{8f_1f_2}{f_3(-2f_4 + f_1f_3f_2' + f_2(f_3f_1' + f_1f_3'))} \Big|_{\tilde{r}=\tilde{r}_{min}} \tag{4.7}$$

The approximate analytic solution (4.7) can be used to fix the boundary conditions for a numerical shooting technique at $\tilde{r} = \tilde{r}_{min} + \delta$ for small values of δ .

A crucial point is that due to the infrared divergency of the perturbative solution, (2.25)-(2.32), this is not valid below a certain radial distance $\tilde{r}_{IR}(\epsilon_*)$ above the origin ($\tilde{r} = 0$). The probe reflects that by having its tension vanishing at $\tilde{r}_{IR}(\epsilon_*)$ but in fact it is the Jacobian $\left| \frac{\partial \tilde{\sigma}}{\partial \tilde{r}} \right|$ which is vanishing at this value of the radial coordinate. As one may expect if we increase the number of backreacted flavors the radius $\tilde{r}_{IR}(\epsilon)$ grows. Therefore we start losing some of the probe brane embeddings corresponding to low bare masses. Fortunately this effect is somewhat softened by the effect of magnetic catalysis of mass generation which leads to infrared separation of the probe branes (the probe closes at some distance above the horizon). To visualize this behavior in figure 3 we have presented plots of D7-brane embeddings in (r, χ) polar coordinates for a range of different infrared separations ($\tilde{L}_0 = \tilde{r}_{min}$) and different number of backreacted flavors ($\epsilon_* \propto \lambda_* \frac{N_f}{N_c}$).

The first plot corresponds to the absence of backreacted matter studied in [3]. As one can see there are two classes of embeddings: those which asymptote to negative (positive) separation at large \tilde{r} . One can show that [3] only the second class corresponds to stable embeddings. The two classes are separated by a critical embedding (depicted with a red curve in figure 3), which has zero separation at large \tilde{r} (vanishing bare mass) and finite separation in the infrared (dynamically generated mass).

The second and the third plots correspond to small (non-vanishing) values of the parameter ϵ_* . As one can see due to the infrared divergencies some of the embeddings with small separation in the infrared are lost. However the critical embedding is still present and we can study how its separation in the infrared (related to the dynamically generated mass) depends on the number of backreacted flavors.

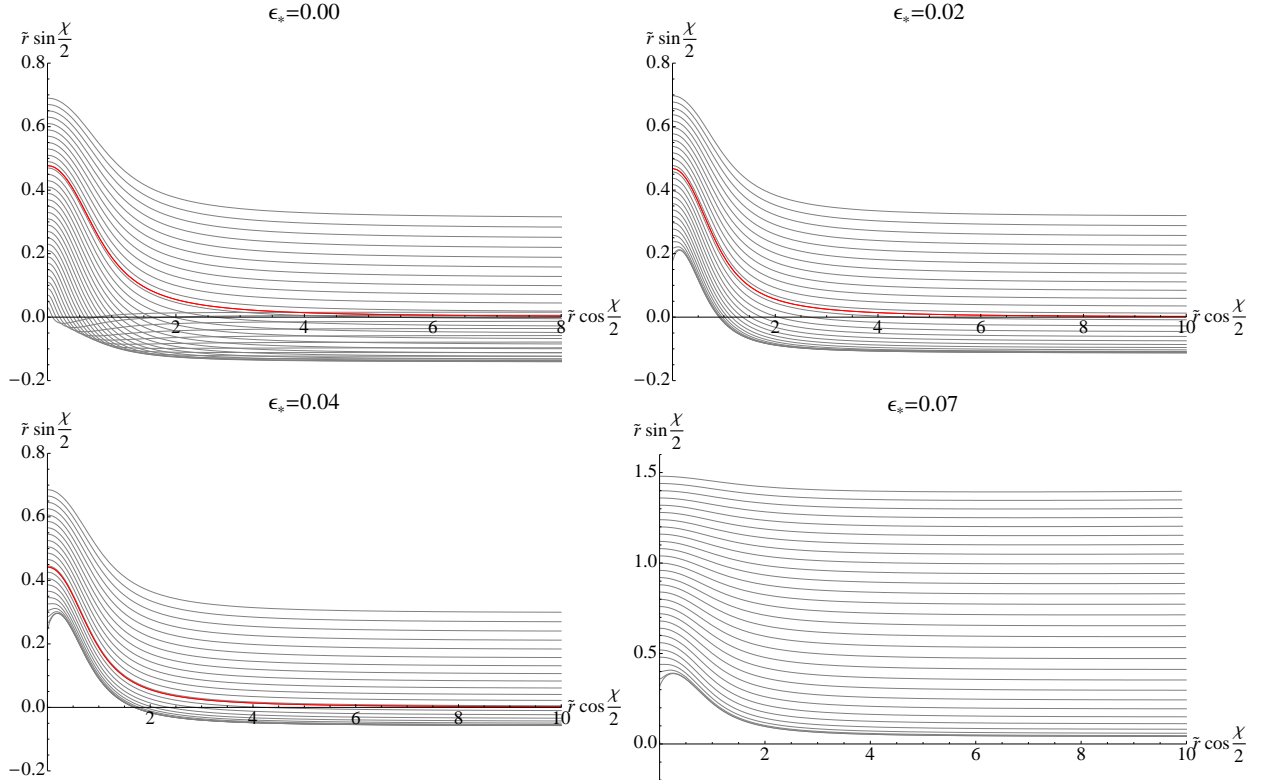


Figure 3: Plots for the profiles of D7-brane embeddings having different infrared separations for various values of the perturbative parameter ϵ_* . The red curves correspond to embeddings with vanishing separation at $r = r_*$, which we interpret as describing fundamental fields with vanishing bare mass and non-vanishing constituent mass.

The last plot in figure 3 corresponds to a sufficiently large number of ϵ_* , at which the radius of the region which is not accessible by the probe brane has increased so much that the embedding with the lowest separation in the infrared asymptotes to positive separation at large \tilde{r} .

At first sight it seems that the validity of the perturbative background is not sufficient to detect a qualitative change of the theory as a function of the parameter ϵ_* . Furthermore unlike the case of the supersymmetric background studied in section 3, we do not have an analogous holographic renormalization procedure. This is why we cannot justify the validity of the AdS/CFT dictionary and in particular (3.27).

Fortunately one can use the properties of the D7-brane embeddings in the infrared, such as the infrared separation \tilde{L}_0 to study the constituent mass of the fundamental fields M_q . Indeed a detailed study of the behavior of the infrared separation $\tilde{L}_0(\epsilon_*)$ of the critical embedding as a function of the parameter ϵ_* is presented in figure 4.

The blue curve corresponds to the function $\tilde{L}_0(\epsilon_*)$. The dashed growing curve corresponds to the radial distance $\tilde{r}_{IR}(\epsilon_*)$ below which the perturbative solution for the background geometry cannot be trusted. The study indicates that for sufficiently large values of ϵ_* the function $\tilde{L}_0(\epsilon_*)$

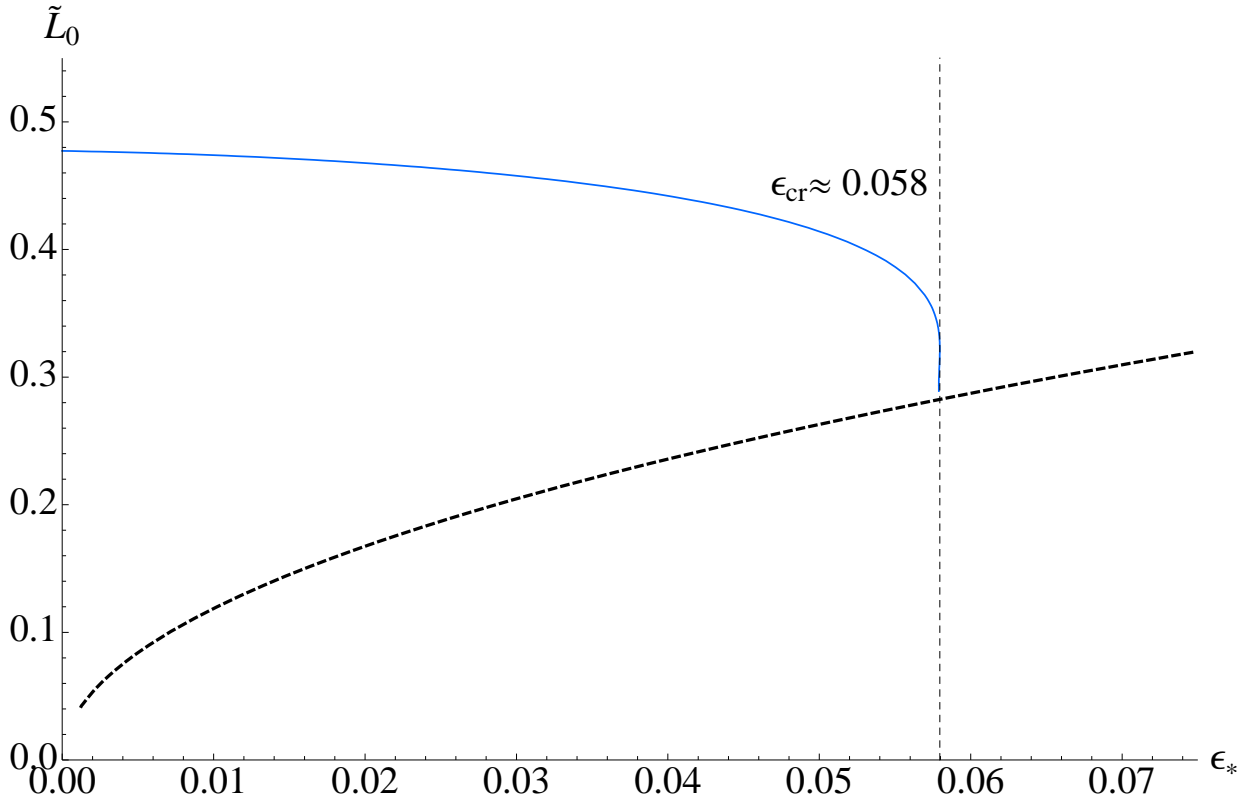


Figure 4: A plot of the infrared separation \tilde{L}_0 (at zero bare mass) versus $\epsilon_* \propto \lambda_* \frac{N_f}{N_c}$.

becomes multivalued through a diverging slope at $\tilde{L}_0 \approx 0.326$. This in turn implies that the critical embedding becomes unstable at this point. The study of the meson spectrum supports that.

It is plausible to interpret the instability of the probe D7-brane as reflecting an instability of the background. Indeed if we consider a single “fiducial” embedding, representative for the smeared massless flavor branes¹⁰, such an embedding would be unstable in the probe limit due to its coupling to the background B -field [22]. Therefore we would expect that the background constructed by smearing many such embeddings would be unstable.

Then a natural question arises. Is there a critical value of the B-field at which the instability is triggered or the background is unstable at any non-vanishing magnetic field? In the probe limit at zero bare mass the only physical scale is the scale corresponding to the non-vanishing B -field (H_*) therefore one would expect that the background is unstable at any $H_* > 0$. On the other side in the backreacted case the dilaton field is running and the theory develops a Landau pole. This suggests that even at vanishing magnetic field the backreacted theory has a physical scale associated to the finite UV cut off needed to keep the relevant energy scales below the Landau pole. Therefore one would expect that there is a finite $H_{cr} > 0$ at which the background becomes unstable.

Let us consider again the physical process described in figure 4. Qualitatively the quantity \tilde{L}_0 can

¹⁰Note that unlike the critical embedding, the smeared massless flavor branes correspond to trivial ($\chi \equiv 0$) embeddings, which are unstable in the presence of non-vanishing B -field

be thought of as proportional to the ratio of the dynamically generated mass of the fundamental fields introduced by the probe D7-brane M_q and the energy scale corresponding to the external magnetic field $\sqrt{H_*}$, namely $\tilde{L}_0 \propto M_q/\sqrt{H_*}$. At any fixed value of ϵ_* we have three independent energy scales: M_q, H_* & H_{cr} . In order to compare states at different values of ϵ_* we will keep the dynamically generated mass of the quarks fixed. The data in figure 4 suggests that as we increase ϵ_* the value of \tilde{L}_0 decreases. At fixed value of M_q this is equivalent of increasing the external magnetic field H_* . Assuming that the critical value H_{cr} varies slowly enough with ϵ_* we conclude that at sufficiently large values of $\epsilon_* \geq \epsilon_{cr}$ the external magnetic field H_* is $H_* \geq H_{cr}$ and the gravitational background is unstable. It is plausible to interpret the instability of the probe D7-brane associated to the diverging slope of $\tilde{L}_0(\epsilon_*)$ in figure 4 as reflecting an instability of the gravitational background for $H_* \geq H_{cr}$.¹¹

Note that the limited validity of our perturbative solution in the deep IR prevent us from directly studying the stability of the background. For example by studying the spectrum of minimally coupled scalar field. It would be interesting to address this problem at finite temperature, where the IR behavior of the supergravity solution is regularized by the non-extremal horizon. We leave such studies for future work.

The instability of the probe D7-brane could be the sign of a “new” physical effect, called “superconducting vacuum”¹². According to [23], the quantum vacuum (i.e., an empty space) may become a superconductor (in the usual electromagnetic sense) under a strong enough magnetic field. This magnetic field forces the electrically charged vector mesons to condense via a tachyonic instability, which in turn implies electromagnetic superconductivity. Calculations in a variety of models, supporting this idea, can be found in [24, 25, 26].

4.2 Meson spectrum

In this section we analyze part of the spectrum of meson like excitations of the dual gauge theory. To this end we perform a semi-classical quantization of the probe D7-brane embeddings studied in section 4.1. In order to obtain the spectrum of the corresponding quantum fluctuations we expand systematically the effective action of the probe D7-brane to second order in α' .

4.2.1 Quadratic fluctuations.

For a detailed study of the light meson spectrum of the theory we need to consider the quadratic fluctuations of a D7-brane and study the corresponding normal modes, [11]. The relevant pieces of the action are

$$\frac{S}{T_7} = - \int d^8x e^{\Phi} \sqrt{-\det \left[G_{ab} + e^{-\frac{\Phi}{2}} (B_{ab} + F_{ab}) \right]} + \int P[\mathcal{C}_{(8)} - F_{(2)} \wedge \mathcal{C}_{(6)} + \frac{1}{2} F_{(2)} \wedge F_{(2)} \wedge \mathcal{C}_{(4)}], \quad (4.8)$$

where $\mathcal{C}_{(4)}, \mathcal{C}_{(6)}$ & $\mathcal{C}_{(8)}$ are defined by:

$$\mathcal{C}_{(4)} \equiv C_{(4)} - C_{(2)} \wedge B_{(2)}, \quad \mathcal{C}_{(6)} \equiv C_{(6)} - B_{(2)} \wedge \tilde{C}_{(4)}, \quad \mathcal{C}_{(8)} \equiv C_{(8)} - B_{(2)} \wedge C_{(6)} \quad (4.9)$$

¹¹However we should point out that though plausible our studies based only on a probe brane calculation alone are not conclusive.

¹²We thank Maxim Chernodub for pointing out to us this possible interpretation.

and $\tilde{C}_{(4)}$ is the magnetic dual of the RR potential $C_{(4)}$

$$\tilde{C}_{(4)} = -\frac{1}{32} Q_c \sin \theta \cos^4 \frac{\chi}{2} d\theta \wedge d\varphi \wedge d\psi \wedge d\tau, \quad (4.10)$$

We will consider fluctuations of the form

$$\chi = \chi_0(\sigma) + 2\pi\alpha' \delta\chi(\xi^a) \quad \& \quad \tau = 2\pi\alpha' \delta\tau(\xi^a), \quad (4.11)$$

where the indices $a, b = 0, 1, \dots, 7$ run along the worldvolume of the D7-brane and expand (4.8) to second order in α' . Before presenting the relevant terms in this expansion it is convenient to introduce S & J , which are symmetric & antisymmetric matrices respectively, in the following way

$$\|E_{ab}^0\|^{-1} = S + J. \quad (4.12)$$

The non-zero elements of those matrices are

$$\begin{aligned} -S^{tt} = S^{11} = G_{11}^{-1}, \quad S^{22} = S^{33} = \frac{G_{22}}{G_{22}^2 + e^{-\Phi} H^2}, \quad S^{\sigma\sigma} = G_{\sigma\sigma}^{-1}, \quad S^{\theta\theta} = G_{\theta\theta}^{-1}, \\ S^{\varphi\varphi} = \frac{G_{\psi\psi}}{G_{\varphi\varphi} G_{\psi\psi} - G_{\varphi\psi}^2}, \quad S^{\varphi\psi} = -\frac{G_{\varphi\psi}}{G_{\varphi\varphi} G_{\psi\psi} - G_{\varphi\psi}^2}, \quad S^{\psi\psi} = \frac{G_{\varphi\varphi}}{G_{\varphi\varphi} G_{\psi\psi} - G_{\varphi\psi}^2}, \end{aligned} \quad (4.13)$$

$$J^{ab} = \frac{e^{-\frac{\Phi}{2}} H}{G_{22}^2 + e^{-\Phi} H^2} (\delta_3^a \delta_2^b - \delta_3^b \delta_2^a), \quad (4.14)$$

with

$$\begin{aligned} G_{11} = g_{11}^{(0)}, \quad G_{22} = g_{22}^{(0)}, \quad G_{\sigma\sigma} = g_{\sigma\sigma}^{(0)} + g_{\chi\chi}^{(0)} \chi_0'(\sigma)^2, \\ G_{\theta\theta} = g_{\theta\theta}^{(0)}, \quad G_{\psi\psi} = g_{\psi\psi}^{(0)}, \quad G_{\varphi\psi} = g_{\varphi\psi}^{(0)}, \quad G_{\varphi\varphi} = g_{\varphi\varphi}^{(0)}. \end{aligned} \quad (4.15)$$

The second order terms in α' expansion of the action (4.8) are

$$\begin{aligned} -\mathcal{L}_{\delta\tau\delta\tau}^{(2)} &= \frac{T_7}{2} e^\Phi \sqrt{-E_0} \left[g_{\tau\tau}^{(0)} - g_{\varphi\tau}^{(0)2} S^{\varphi\varphi} - 2g_{\varphi\tau}^{(0)} g_{\psi\tau}^{(0)} S^{\varphi\psi} - g_{\psi\tau}^{(0)2} S^{\psi\psi} \right] S^{ab} \partial_a \delta\tau \partial_b \delta\tau, \\ -\mathcal{L}_{\delta\chi\delta\chi}^{(2)} &= \frac{T_7}{2} e^\Phi \sqrt{-E_0} g_{\chi\chi}^{(0)} \left[1 - g_{\chi\chi}^{(0)} S^{\sigma\sigma} \chi_0'(\sigma)^2 \right] S^{ab} \partial_a \delta\chi \partial_b \delta\chi + \frac{1}{2} \tilde{f}(\sigma) \delta\chi^2, \\ -\mathcal{L}_{\delta\chi\delta\tau}^{(2)} &= T_7 \mathcal{J}^a \delta\chi \partial_a \delta\tau, \quad \mathcal{L}_{AA}^{(2)} = \frac{T_7}{4} \sqrt{-E_0} S^{aa'} S^{bb'} F_{ab} F_{a'b'} + \frac{T_7}{2} P[\mathcal{C}_4] \epsilon^{mnop} F_{mn} F_{op}, \\ -\mathcal{L}_{\delta\chi A}^{(2)} &= f(\sigma) \delta\chi F_{34} \quad \& \quad \mathcal{L}_{\delta\tau A}^{(2)} = \frac{T_7}{32} Q_c H_* \partial_\sigma \left[\cos^4 \frac{\chi_0(\sigma)}{2} \right] \delta\tau F_{12}. \end{aligned} \quad (4.16)$$

where the indices m, n, o, p run in the transverse directions of the D3-branes. The auxiliary functions f, g & \mathcal{J}^a , appearing in the above equations, are defined as follows

$$\begin{aligned}
f(\sigma) &\equiv T_7 \partial_\sigma \left[e^{\frac{\Phi}{2}} \sqrt{-E_0} J^{23} g_{\chi\chi}^{(0)} S^{\sigma\sigma} \chi'_0(\sigma) \right] - T_7 e^{-\frac{\Phi}{2}} J^{23} \partial_\chi \sqrt{-E_0} - \partial_\chi \mathcal{L}_{\text{WZ}}^{(0)}, \\
\tilde{f}(\sigma) &\equiv \partial_\chi^2 \mathcal{L}^{(0)} - T_7 \partial_\sigma \left[e^\Phi g_{\chi\chi}^{(0)} S^{\sigma\sigma} \chi'_0(\sigma) \partial_\chi \sqrt{-E_0} \right], \\
\mathcal{J}^a &\equiv e^\phi S^{ab} \partial_\chi (\sqrt{-E_0}) g_{b\tau}^{(0)} - e^\Phi \sqrt{-E_0} S^{aa'} \partial_\chi g_{a'b'} S^{b'c} g_{c\tau}^{(0)} - \partial_\sigma (e^\Phi S^{ab} \sqrt{-E_0} g_{\chi\chi}^{(0)}) \chi' g_{b\tau}^{(0)},
\end{aligned} \tag{4.17}$$

where $\mathcal{L}^{(0)}, \mathcal{L}_{\text{WZ}}^{(0)}$ are the complete classical lagrangian of the probe brane (4.2) and the C_6 contribution of the Wess-Zumino part respectively. Note that the function \mathcal{J}^a is non-vanishing only for $a = \phi, \psi$.

Note that if one restricts the fluctuating modes to depend only on the time and the holographic directions the coupling term in the effective lagrangian vanish and we can consistently focus only on the fluctuations along χ .

4.2.2 Fluctuations along χ

We consider the ansatz

$$\delta\chi = e^{i\omega t} \eta(\sigma), \quad \delta\tau = 0 \quad \& \quad A_\mu = 0. \tag{4.18}$$

The only relevant part of the effective action is the term $\mathcal{L}_{\delta\chi\delta\chi}^{(2)}$. We find it convenient to use the radial coordinate $r(\sigma)$ related to σ via equation (2.25). Using the dimensionless notation defined in equations (4.3) and (4.6) we obtain the equation of motion for $\eta(\tilde{r})$

$$\partial_{\tilde{r}} \left[\frac{\tilde{\mathcal{L}}_{\text{DBI}}^{(0)} f_3^2}{(1 + f_3^2 \chi'^2)^2} \partial_{\tilde{r}} \eta \right] + \left[\frac{\tilde{\mathcal{L}}_{\text{DBI}}^{(0)} f_5^2}{1 + f_3^2 \chi'^2} \tilde{\omega}^2 - \left[\partial_\chi^2 \tilde{\mathcal{L}}^{(0)} - \partial_{\tilde{r}} \left(\frac{f_3^2 \chi'}{1 + f_3^2 \chi'^2} \partial_\chi \tilde{\mathcal{L}}_{\text{DBI}}^{(0)} \right) \right] \right] \eta = 0, \tag{4.19}$$

where

$$\tilde{\omega}^2 \equiv \frac{Q_c}{4r_m^2} \omega^2, \quad f_5(\tilde{r}) \equiv \frac{\tilde{S}(\tilde{r})}{2\tilde{r}^2}. \tag{4.20}$$

In order to solve numerically (4.19) we need to impose proper boundary conditions at $\tilde{r} = \tilde{r}_{\min} = \tilde{L}_0$. Using (4.7) for the classical embedding one obtains the following asymptotic form of (4.19)

$$\eta''(\tilde{r}) + \frac{3}{\tilde{r} - \tilde{r}_{\min}} \eta'(\tilde{r}) + \frac{3}{4} \frac{1}{(\tilde{r} - \tilde{r}_{\min})^2} \eta(\tilde{r}) = 0. \tag{4.21}$$

The general solution of equation (4.21) is

$$\eta(\tilde{r}) = \frac{C_1}{(\tilde{r} - \tilde{r}_{\min})^{\frac{1}{2}}} + \frac{C_2}{(\tilde{r} - \tilde{r}_{\min})^{\frac{3}{2}}}. \tag{4.22}$$

Requiring renormalizability for $\eta(\tilde{r})$

$$\int_{\tilde{r}_{min}}^{\tilde{r}_*} d\tilde{r} \sqrt{-\tilde{E}^{(0)}} |\eta(\tilde{r})|^2 < \infty, \quad (4.23)$$

and the fact that $\sqrt{-\tilde{E}^{(0)}} \sim (\tilde{r} - \tilde{r}_{min})$ one can see that C_2 should vanish. This suggests the following substitution in equation (4.19)

$$\eta(\tilde{r}) = \frac{\zeta(\tilde{r})}{\sqrt{\tilde{r} - \tilde{r}_{min}}}, \quad (4.24)$$

where the function $\zeta(\tilde{r})$ is analytic near \tilde{r}_{min} . The resulting equation of motion for $\zeta(\tilde{r})$ is of the form

$$\zeta''(\tilde{r}) + \left(C_1 - \frac{1}{\tilde{r} - \tilde{r}_{min}} \right) \zeta'(\tilde{r}) + \left(C_0 + B^2 \tilde{\omega}^2 - \frac{C_1}{\tilde{r} - \tilde{r}_{min}} + \frac{3}{4} \frac{1}{(\tilde{r} - \tilde{r}_{min})^2} \right) \zeta(\tilde{r}) = 0, \quad (4.25)$$

where C_0, C_1 & B are functions of \tilde{r} and $\chi(\tilde{r})$ regular at $\tilde{r} = \tilde{r}_{min}$. Equation (4.25) has predetermined boundary conditions at \tilde{r}_{min} . Therefore one can expand $\zeta(\tilde{r})$ near \tilde{r}_{min} and solve equation (4.25) order by order. The obtained approximate solution for $\zeta(\tilde{r})$ can be used to fix the boundary conditions for a numerical shooting technique. The resulting numerical solution depends on the parameter $\tilde{\omega}$. Imposing Dirichlet boundary condition at $\tilde{r} = \tilde{r}_*$ quantizes the spectrum of $\tilde{\omega}$.

We used the procedure outlined above to generate plots of the first three excited states of the spectrum as a function of the parameter ϵ_* . The resulting plots are presented in figure 5. One can see that the ground state becomes tachyonic exactly at the critical value of $\epsilon_* \approx 0.058$ where the slope of \tilde{L}_0 versus ϵ_* in figure 4 diverges. This confirms that at this point the probe branes become unstable. As we commented in subsection 4.1 we interpret this instability as reflecting an instability of the background. This suggests that the dual gauge theory is unstable for sufficiently strong magnetic fields. This is to be expected because the backreacted massless flavors are in a phase with vanishing constituent mass which is disfavored by the external magnetic field.

5. Conclusions

In this paper we propose a string theory dual to a 1+3 $SU(N_c)$ $\mathcal{N} = 4$ SYM theory coupled to N_f massless fundamental flavors in an external magnetic field. Our motivation is to undertake the first steps towards an unquenched holographic description of magnetic catalysis of mass generation. By construction, our background corresponds to a phase of the flavored theory with vanishing constituent mass. This phase is disfavored by the external magnetic field, therefore one would expect that for sufficiently strong B -field the supergravity background would become unstable. Unfortunately the infrared singularity of our perturbative solution prevents us from directly studying the stability of the background by studying the spectrum of its quasi-normal modes. To circumnavigate this limitation we study the properties of an additional probe D7-brane.

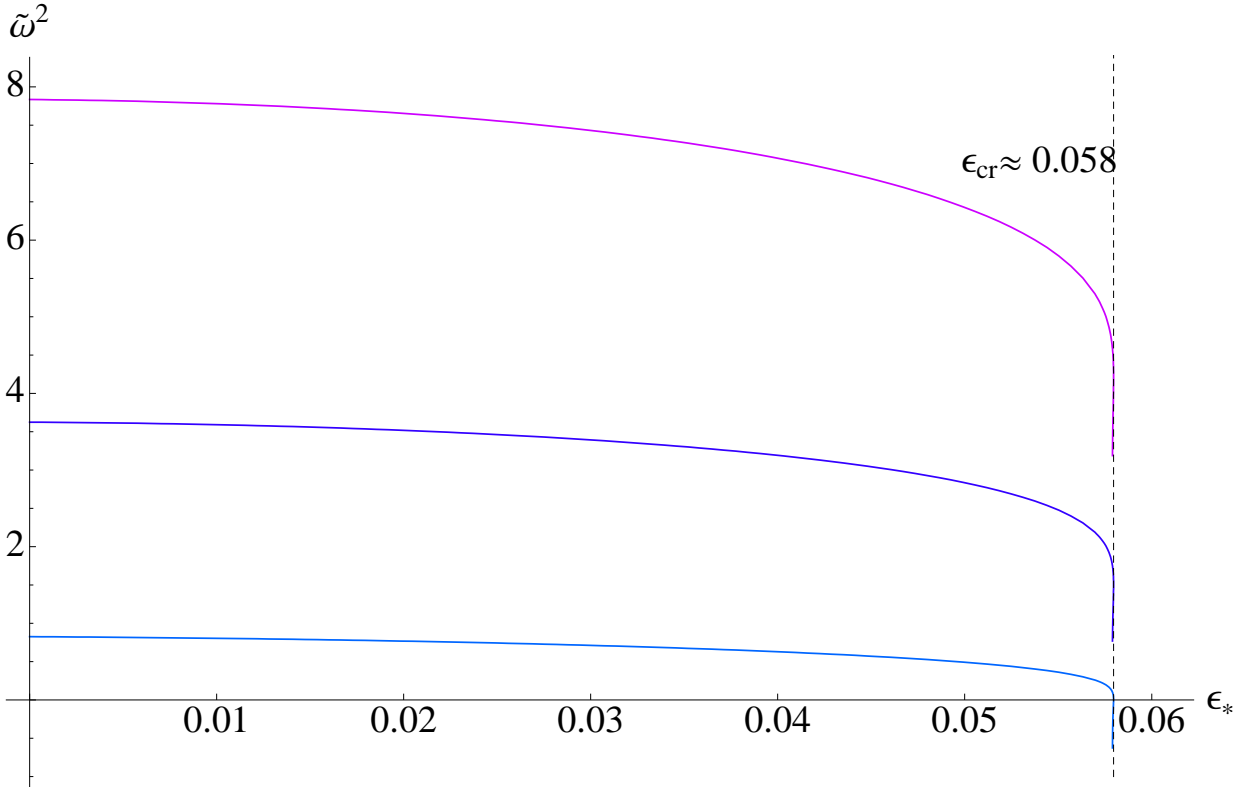


Figure 5: Plots of the first three excited states of $\tilde{\omega}$ versus $\epsilon_* \propto N_f/N_c$. One can see that at the critical value $\epsilon_* \approx 0.058$ the ground state is tachyonic.

In Section 3.1 we study the properties of a supersymmetric probe D7-brane in the limit of vanishing B -field. In this way our background reduces to the supersymmetric one obtained in [15]. We consider a holographic renormalization of the probe brane “on-shell” action in the spirit of [21], but in the case with backreacted flavors. Our studies reveal a remarkable factorization of the dependence of the “on-shell” action on the perturbative parameter counting the number of backreacted flavors (ϵ_*). This factorization suggests that the holographic renormalization performed in [21] can be implemented, at least formally, for the background [15]. Next, a systematic expansion in ϵ_* , for $\epsilon_* \ll 1$ & keeping the finite cut off of the theory sufficiently far bellow the Landau pole, provides a regime of validity of the renormalization procedure. This suggests that the usual AdS/CFT dictionary holds at the UV scale fixed by the finite cut off.

In Section 3.2 we move one step forward our study and introduce a non-supersymmetric probe D7-brane to the supersymmetric background of [15]. This probe brane has a fixed $U(1)$ worldvolume gauge field corresponding to an external magnetic field coupled to the fundamental fields introduced by the probe brane only. Using the AdS/CFT dictionary proposed in the previous section we study the effect of mass generation and its dependence on the number of backreacted fundamental flavors. Qualitatively the physical picture remains the same compared to the one without backreacted flavors, [3]. We contrast these results to those of a magnetic field coupling to all fundamental

degrees of freedom.

Finally in Section 4 we consider a D7-brane probe in the supergravity background obtained in Section 2. Now the B -field, corresponding to an external magnetic field, couples to both the probe and the backreacted fundamental degrees of freedom. The study of the meson spectrum shows that for sufficiently strong magnetic field the probe brane becomes unstable. It is plausible to interpret this instability as reflecting an instability of the supergravity background.¹³ As commented above this is anticipated since the external magnetic field disfavors a phase with vanishing constituent mass of the fundamental fields. We speculate that the stable phase at vanishing bare mass would correspond to a supergravity background obtained by smearing “fiducial” embeddings with a non-trivial profile along the radial coordinate having finite separation in the infrared corresponding to dynamically generated constituent mass. The construction of such a background is one of the main directions for future studies that we intend to pursue.

A possible way to improve the IR properties of the gravity dual constructed in Section 2 is to consider the non-extremal case, when the zeroth order solution is the $\text{AdS}_5 \times S^5$ black hole. In this case it would be possible to study directly the spectrum of quasi-normal modes of the background and verify the anticipated instability for sufficiently strong magnetic field. One could also introduce an additional probe brane and perform a study analogous to the one considered in Section 4.2 of the present work. Naturally, one would expect that such a probe would become unstable when the energy scale of the magnetic field is sufficiently larger than the energy scale of the finite temperature. One can then compare the critical parameters obtained from studying the spectrum of quasi-normal modes of the background and from studying fluctuations of the probe brane. Such a study could provide an indirect check of the interpretation of the instability of the probe brane considered in Section 4.2.¹⁴ We leave such studies for a future work.

6. Acknowledgments

V. F. and D. Z. would like to thank F. Bigazzi, M. Chernodub, A. Cotrone, J. Erdmenger, P. Kerner, I. Kirsch, S. Lin, R. Meyer, J. Mas, C. Nunez, A Paredes, A. Ramallo & J. Shock for useful comments and suggestions. D.Z. is funded by the FCT fellowship SFRH/BPD/62888/2009. Centro de Física do Porto is partially funded by FCT through the projects PTDC/FIS/099293/2008 & CERN/FP/109306/2009. The work of V. F. is funded by an INSPIRE IRCSET-Marie Curie International Mobility Fellowship. V. F. would like to thank the organizers of the GGI Workshop “Large-N Gauge Theories” for hospitality during the final stages of this project.

¹³However we should point out that though plausible our studies based on a probe brane calculation alone are not conclusive.

¹⁴We thank Aldo Cotrone for comments on this point.

A. Equations of motion

The equations of motion produced from (2.1) are [27]

$$\begin{aligned}
R_{\mu\nu} = & \frac{1}{2} \partial_\mu \Phi \partial_\nu \Phi + \frac{1}{2} e^{2\Phi} F_\mu^{(1)} F_\nu^{(1)} + \frac{1}{4} \frac{1}{5!} \left[5 F_{\mu\rho\sigma\alpha\beta}^{(5)} F_\nu^{(5)\rho\sigma\alpha\beta} - \frac{1}{2} g_{\mu\nu} F_{(5)}^2 \right] \\
& + \frac{1}{2} \frac{1}{3!} e^\Phi \left[3 F_{\mu\rho\sigma}^{(3)} F_\nu^{(3)\rho\sigma} - \frac{1}{4} g_{\mu\nu} F_{(3)}^2 \right] + \frac{1}{2} \frac{1}{3!} e^{-\Phi} \left[3 H_{\mu\rho\sigma}^{(3)} H_\nu^{(3)\rho\sigma} - \frac{1}{4} g_{\mu\nu} H_{(3)}^2 \right] \\
& + \left[T_{fl} - \frac{1}{8} g_{\mu\nu} T_{fl}^2 \right], \tag{A.1}
\end{aligned}$$

$$d[\star d\Phi] = e^{2\Phi} F_{(1)} \wedge \star F_{(1)} + \frac{1}{2} e^\Phi F_{(3)} \wedge \star F_{(3)} - \frac{1}{2} e^{-\Phi} H_{(3)} \wedge \star H_{(3)} - 2\kappa^2 \frac{\delta S_{fl}}{\delta \Phi}, \tag{A.2}$$

$$d[e^{2\Phi} \star F_{(1)}] = -e^\Phi H_{(3)} \wedge \star F_{(3)} - \frac{1}{24} \mathcal{F}^4 \wedge \Omega_2, \tag{A.3}$$

$$d[e^\Phi \star F_{(3)}] = -H_{(3)} \wedge F_{(5)} + \frac{1}{6} \mathcal{F}^3 \wedge \Omega_2, \tag{A.4}$$

$$d[\star F_{(5)}] = dF_{(5)} = H_{(3)} \wedge F_{(3)} - \frac{1}{2} \mathcal{F}^2 \wedge \Omega_2, \tag{A.5}$$

$$d[e^{-\Phi} \star H_{(3)}] = e^\Phi F_{(1)} \wedge \star F_{(3)} - F_{(5)} \wedge F_{(3)} - \frac{\delta S_{fl}^{(\text{DBI})}}{\delta \mathcal{F}}. \tag{A.6}$$

where the last term in (A.6) is an eight form and denotes the derivative of the smeared DBI action with respect to \mathcal{F}

$$\int d^8x e^\Phi \sqrt{-\det(\hat{G} + e^{-\Phi/2} \mathcal{F})} \rightarrow \int d^{10}x e^\Phi \sqrt{-\det(G + e^{-\Phi/2} \mathcal{F})} |\Omega_2| \tag{A.7}$$

The symbol $|\Omega_2|$ that appears in (A.7) denotes the modulus of the smearing form and has the following expression

$$|\Omega_2| = 2 \frac{2Q_f}{\sqrt{h} S^2}. \tag{A.8}$$

The Bianchi identities for all the forms of the background are

$$dF_{(1)} = -g_s \Omega_2, \tag{A.9}$$

$$dF_{(3)} = H_{(3)} \wedge F_{(1)} - g_s \mathcal{F} \wedge \Omega_2, \tag{A.10}$$

$$dH_{(3)} = 0. \tag{A.11}$$

The Bianchi identities and the equations of motion for the worldvolume gauge fields are

$$d\mathcal{F} = H_3 \quad \& \quad d \left[\frac{\delta S_{fl}}{\delta \mathcal{F}} \right] = 0. \tag{A.12}$$

Plugging the ansatz of (2.7) in the Bianchi identities (A.9), (A.10) and (A.11) as well as the equations of motion (A.3) and (A.5), trivially satisfies them all. The equations of motion for F_3 & H_3 , namely (A.4) & (A.6), will give us (2.13) & (2.21) respectively.

The equation of motion for the dilaton, namely (A.2), will give us (2.20). The contribution from the last term in (A.2) is the following

$$2\kappa^2 \frac{\delta S_{fl}}{\delta \Phi} = -\frac{4e^\Phi Q_f}{\sqrt{h} S^2} \frac{1 + \frac{e^{-\Phi} H^2 h}{2b^2}}{\sqrt{1 + \frac{e^{-\Phi} H^2 h}{b^2}}}. \quad (\text{A.13})$$

The Einstein equations, namely (A.1), will give us (2.16), (2.17), (2.18) & (2.19) together with the constraint (2.22). This last one is coming from the 44 (frame) component of the Einstein equations. The contribution from T_{fl} that appears in (A.1) is the following

$$T_{\mu\nu}^{fl} = \frac{2\kappa^2}{\sqrt{-g}} \frac{\delta S_{fl}}{\delta g^{\mu\nu}} = \frac{1}{2} g_s e^\Phi \sqrt{-\mathcal{E}} \left[\mathcal{S}_{\mu\nu} |\Omega_2| - \frac{2}{|\Omega_2|} \Omega_{\rho\mu}^{(2)} \Omega_{\nu}^{(2)\rho} \right], \quad (\text{A.14})$$

with

$$\mathcal{E}_{\mu\nu} = \eta_{\mu\nu} + e^{-\frac{\Phi}{2}} \frac{H \sqrt{h}}{b} (\delta_2^\mu \delta_3^\nu - \delta_2^\nu \delta_3^\mu), \quad (\mu, \nu = 0, 1, \dots, 9) \quad (\text{A.15})$$

and \mathcal{S} is the symmetric part of the inverse of \mathcal{E}

$$\mathcal{S}_{\mu\nu} = \text{diag}\left\{-1, 1, \frac{1}{1 + e^{-\Phi} \frac{H^2 h}{b^2}}, \frac{1}{1 + e^{-\Phi} \frac{H^2 h}{b^2}}, 1, 1, 1, 1, 1, 1\right\}. \quad (\text{A.16})$$

Finally for the worldvolume gauge fields, we have the first of the equations in (A.12) trivially satisfied while the second splits into

$$d \left[\frac{\delta S_{fl}^{(\text{DBI})}}{\delta \mathcal{F}} \right] + d \left[\frac{\delta S_{fl}^{(\text{WZ})}}{\delta \mathcal{F}} \right] = 0. \quad (\text{A.17})$$

The first term in (A.17) can be easily evaluated if one differentiates (A.6) and plugs in the ansatz (2.7). One can show that it is of order $d[\mathcal{O}(dA)]$. The second term is proportional to the expression

$$d [C_{(6)} \wedge \Omega_2 + \mathcal{O}(dA)] \rightarrow d[\mathcal{O}(dA)]. \quad (\text{A.18})$$

The bottom line is that the whole expression in (A.12) is of order $d[\mathcal{O}(dA)]$ and hence one can consistently set the D-brane worldvolume gauge field to zero ($A \equiv 0$).

B. Technical details

In this appendix we will present some technical details on the computations of Section 3.

B.1 Exact On-Shell Action

The ‘‘on-shell’’ action $-S_{cl}/(\mathcal{N}\alpha'^2)$ of a supersymmetric embedding with bare mass parameter e^{ρ_q} in the supergravity background described by equations (3.17)–(3.20) is given by

$$\int_{\rho_q}^{\rho_*} d\rho \frac{e^{\Phi_*}(e^{2\rho} - e^{2\rho_q})[6\epsilon_*(e^{2\rho} - e^{2\rho_q})(1 + \epsilon_*(\frac{1}{6} + \rho_* - \rho)) + 4(1 + \epsilon_*(\rho_* - \rho))(6e^{2\rho}(1 + \epsilon_*(\rho_* - \rho) + \epsilon_*e^{2\rho_q}))]}{32 \times 6(1 + \epsilon_*(\frac{1}{6} + \rho_* - \rho))^{\frac{1}{3}}(1 + \epsilon_*(\rho_* - \rho))^2}. \quad (\text{B.1})$$

The definite integral in (B.1) can be solved in a closed form using the relatively simple dependence on the parameter e^{ρ_q} . To this end one defines $m_q \equiv e^{\rho_q}$ and takes the second derivative with respect to $m_q^2 = e^{2\rho_q}$

$$\frac{\partial^2 S_{cl}[\rho_*, m_q^2]}{\partial(m_q^2)^2} = -\mathcal{N}\alpha'^2 \frac{e^{\Phi_*}}{16} \left(1 + \frac{\epsilon_*}{6}\right)^{\frac{2}{3}}. \quad (\text{B.2})$$

Furthermore equation (B.1) suggests that $S_{cl}|_{\rho_q=\rho_*} = 0$ and one can verify that $\partial_{(m_q)^2} S_{cl}|_{\rho_*=\rho_q} = 0$. Therefore we can integrate (B.2) and obtain the following expression for the classical action

$$-\frac{S_{cl}}{\mathcal{N}\alpha'^2} = \frac{e^{\Phi_*}}{32} \left(1 + \frac{\epsilon_*}{6}\right)^{\frac{2}{3}} (e^{2\rho_*} - e^{2\rho_q})^2, \quad (\text{B.3})$$

which is exactly (3.23).

B.2 The Function h

In order to evaluate the effective action from (3.29) we need to integrate the equation of motion for $h(\rho)$ in (3.20). Changing variables to dimensionless ones along (3.30), the equation of motion for $h(\tilde{\rho})$ becomes

$$\frac{\partial h}{\partial \tilde{\rho}} = -4e^{-4\tilde{\rho}} \left[1 + \epsilon_* \left(\frac{1}{6} + \tilde{\rho}_* - \tilde{\rho}\right)\right]^{-\frac{2}{3}}. \quad (\text{B.4})$$

A short integral expression can be given in terms of $x \equiv 1/\epsilon + 1/6 + \tilde{\rho}_* - \tilde{\rho}$

$$h(x) = e^{-4\tilde{\rho}_*} \left(1 + \frac{4e^{-\frac{4}{\epsilon} - \frac{2}{3}}}{\epsilon_*^{\frac{2}{3}}} \int_{x_*}^x dx \frac{e^{4x}}{x^{\frac{2}{3}}}\right) \quad \text{with} \quad x_* \equiv x(\tilde{\rho}_*) = \frac{1}{\epsilon_*} + \frac{1}{6}. \quad (\text{B.5})$$

The constant of integration in (B.5) is fixed by requiring $h(\tilde{\rho}_*) = e^{-4\tilde{\rho}_*}$. Using that

$$\int dx \frac{e^{4x}}{x^{\frac{2}{3}}} = \frac{e^{i\frac{2\pi}{3}}}{2^{\frac{2}{3}}} \left[\Gamma\left(\frac{1}{3}, -4x\right) - \Gamma\left(\frac{1}{3}\right)\right] + \text{const}, \quad (\text{B.6})$$

where $\Gamma(a)$ and $\Gamma(a, z)$ are the complete and incomplete gamma functions¹⁵, we have

$$h(\tilde{\rho}) = e^{-4\tilde{\rho}_*} \left[1 + \frac{4e^{-\frac{4}{\epsilon} - \frac{2}{3}(1-i\pi)}}{(2\epsilon_*)^{\frac{2}{3}}} \left[\Gamma\left(\frac{1}{3}, -\frac{4}{\epsilon_*} - \frac{2}{3} - 4(\tilde{\rho}_* - \tilde{\rho})\right) - \Gamma\left(\frac{1}{3}, -\frac{4}{\epsilon_*} - \frac{2}{3}\right)\right]\right]. \quad (\text{B.7})$$

¹⁵Note that the right-hand side of equation (B.6) is real for $x > 0$.

Note that for $\tilde{\rho} \in (-\infty, \tilde{\rho}_*)$ & $\epsilon_* > 0$ $h(\tilde{\rho})$ is real.

References

- [1] J. M. Maldacena, Adv. Theor. Math. Phys. **2**, 231-252 (1998). [hep-th/9711200].
- [2] V. P. Gusynin, V. A. Miransky and I. A. Shovkovy, Phys. Rev. Lett. **73**, 3499 (1994) [Erratum-ibid. **76**, 1005 (1996)] [arXiv:hep-ph/9405262].
V. P. Gusynin, V. A. Miransky and I. A. Shovkovy, Phys. Lett. B **349**, 477 (1995) [arXiv:hep-ph/9412257].
K. G. Klimenko, Theor. Math. Phys. **89**, 1161 (1992) [Teor. Mat. Fiz. **89**, 211 (1991)].
K. G. Klimenko, Z. Phys. C **54**, 323 (1992).
K. G. Klimenko, Theor. Math. Phys. **90**, 1 (1992) [Teor. Mat. Fiz. **90**, 3 (1992)].
- [3] V. G. Filev, C. V. Johnson, R. C. Rashkov and K. S. Viswanathan, JHEP **0710**, 019 (2007) [arXiv:hep-th/0701001].
- [4] J. Erdmenger, N. Evans, I. Kirsch and E. Threlfall, Eur. Phys. J. A **35**, 81 (2008) [arXiv:0711.4467 []].
- [5] V. G. Filev and R. C. Raskov, Adv. High Energy Phys. **2010** (2010) 473206 [arXiv:1010.0444 []].
- [6] A. Kehagias, Phys. Lett. **B435**, 337-342 (1998). [hep-th/9805131].
O. Aharony, A. Fayyazuddin and J. M. Maldacena, JHEP **9807**, 013 (1998) [arXiv:hep-th/9806159].
- [7] M. Grana and J. Polchinski, Phys. Rev. D **65**, 126005 (2002) [arXiv:hep-th/0106014].
M. Bertolini, P. Di Vecchia, M. Frau, A. Lerda and R. Marotta, Nucl. Phys. B **621**, 157 (2002) [arXiv:hep-th/0107057].
B. A. Burrington, J. T. Liu, L. A. Pando Zayas and D. Vaman, JHEP **0502**, 022 (2005) [arXiv:hep-th/0406207].
- [8] C. Nunez, A. Paredes, A. V. Ramallo, Adv. High Energy Phys. **2010**, 196714 (2010). [arXiv:1002.1088 [hep-th]].
- [9] A. Karch and E. Katz, JHEP **0206**, 043 (2002) [arXiv:hep-th/0205236].
- [10] F. Bigazzi, A. L. Cotrone, A. Paredes, JHEP **0809**, 048 (2008). [arXiv:0807.0298 [hep-th]].
- [11] M. Kruczenski, D. Mateos, R. C. Myers, D. J. Winters, JHEP **0307**, 049 (2003). [hep-th/0304032].
- [12] F. Bigazzi, A. L. Cotrone, J. Mas, A. Paredes, A. V. Ramallo, J. Tarrío JHEP **0911**, 117 (2009). [arXiv:0909.2865 [hep-th]].
- [13] F. Bigazzi, A. L. Cotrone, J. Tarrío, JHEP **1002**, 083 (2010) [arXiv:0912.3256 [hep-th]].
F. Bigazzi, A. L. Cotrone, JHEP **1008**, 128 (2010) [arXiv:1006.4634 [hep-ph]].
- [14] F. Bigazzi, A. L. Cotrone, J. Mas, D. Mayerson, J. Tarrío, JHEP **1104**, 060 (2011). [arXiv:1101.3560 [hep-th]].

- [15] F. Benini, F. Canoura, S. Cremonesi, C. Nunez, A. V. Ramallo, *JHEP* **0702**, 090 (2007). [hep-th/0612118].
- [16] A. Paredes, *JHEP* **0612**, 032 (2006) [arXiv:hep-th/0610270].
 F. Benini, F. Canoura, S. Cremonesi, C. Nuñez and A. V. Ramallo, *JHEP* **0709**, 109 (2007) [arXiv:0706.1238 [hep-th]].
 R. Casero, C. Nuñez and A. Paredes, *Phys. Rev. D* **77**, 046003 (2008) [arXiv:0709.3421 [hep-th]].
 E. Caceres, R. Flauger, M. Ihl and T. Wrase, *JHEP* **0803**, 020 (2008) [arXiv:0711.4878 [hep-th]].
 F. Canoura, P. Merlatti and A. V. Ramallo, *JHEP* **0805**, 011 (2008) [arXiv:0803.1475 [hep-th]].
 F. Bigazzi, A. L. Cotrone, C. Nuñez and A. Paredes, *Phys. Rev. D* **78**, 114012 (2008) [arXiv:0806.1741 [hep-th]].
 C. Hoyos-Badajoz, C. Nuñez and I. Papadimitriou, *Phys. Rev. D* **78**, 086005 (2008) [arXiv:0807.3039 [hep-th]].
 D. Arean, P. Merlatti, C. Nuñez and A. V. Ramallo, *JHEP* **0812**, 054 (2008) [arXiv:0810.1053 [hep-th]].
 J. Gaillard and J. Schmude, *JHEP* **0901**, 079 (2009) [arXiv:0811.3646 [hep-th]].
 A. V. Ramallo, J. P. Shock and D. Zoakos, *JHEP* **0902**, 001 (2009) [arXiv:0812.1975 [hep-th]].
 F. Bigazzi, A. L. Cotrone, A. Paredes and A. V. Ramallo, *JHEP* **0903**, 153 (2009) [arXiv:0812.3399 [hep-th]].
 F. Bigazzi, A. L. Cotrone, A. Paredes and A. V. Ramallo, *JHEP* **0905**, 034 (2009) [arXiv:0903.4747 [hep-th]].
 J. Gaillard and J. Schmude, *JHEP* **1002**, 032 (2010) [arXiv:0908.0305 [hep-th]].
 C. Nunez, M. Piai and A. Rago, *Phys. Rev. D* **81**, 086001 (2010) [arXiv:0909.0748 [hep-th]].
 D. Arean, E. Conde and A. V. Ramallo, *JHEP* **0912**, 006 (2009) [arXiv:0909.3106 [hep-th]].
 D. Elander, *JHEP* **1003**, 114 (2010). [arXiv:0912.1600 [hep-th]].
 D. Arean, E. Conde, A. V. Ramallo and D. Zoakos, *JHEP* **1006**, 095 (2010). [arXiv:1004.4212 [hep-th]].
 J. Gaillard, D. Martelli, C. Nunez and I. Papadimitriou, *Nucl. Phys. B* **843**, 1 (2011) [arXiv:1004.4638 [hep-th]].
 J. Schmude, [arXiv:1007.1201 [hep-th]].
 E. Conde, J. Gaillard, *Nucl. Phys.* **B848**, 431-473 (2011). [arXiv:1011.1451 [hep-th]].
 E. Caceres, C. Nunez, L. A. Pando-Zayas, *JHEP* **1103**, 054 (2011). [arXiv:1101.4123 [hep-th]].
 D. Elander, J. Gaillard, C. Nunez, M. Piai, [arXiv:1104.3963 [hep-th]].
- [17] I. R. Klebanov and E. Witten, *Nucl. Phys. B* **536**, 199 (1998) [arXiv:hep-th/9807080].
- [18] R. Casero, C. Nunez, A. Paredes, *Phys. Rev. D* **73**, 086005 (2006). [hep-th/0602027].
- [19] F. Bigazzi, R. Casero, A. L. Cotrone, E. Kiritsis, A. Paredes, *JHEP* **0510**, 012 (2005). [hep-th/0505140].
- [20] E. Conde, A. V. Ramallo, [arXiv:1105.6045 [hep-th]].
- [21] A. Karch, A. O'Bannon and K. Skenderis, *JHEP* **0604**, 015 (2006) [arXiv:hep-th/0512125].
- [22] V. G. Filev, *JHEP* **0804**, 088 (2008) [arXiv:0706.3811 [hep-th]].
- [23] M. N. Chernodub, *Phys. Rev. D* **82**, 085011 (2010). [arXiv:1008.1055 [hep-ph]].

- [24] M. N. Chernodub, Phys. Rev. Lett. **106**, 142003 (2011). [arXiv:1101.0117 [hep-ph]].
- [25] V. V. Braguta, P. V. Buividovich, M. N. Chernodub, M. I. Polikarpov, [arXiv:1104.3767 [hep-lat]].
- [26] N. Callebaut, D. Dudal, H. Verschelde, [arXiv:1105.2217 [hep-th]].
- [27] F. Benini, JHEP **0810**, 051 (2008). [arXiv:0710.0374 [hep-th]].